Subduction zone coupling and tectonic block rotations in the North Island, New Zealand

Laura M. Wallace and John Beavan
Institute of Geological and Nuclear Sciences, Lower Hutt, New Zealand

Robert McCaffrey
Department of Earth and Environmental Sciences, Rensselaer Polytechnic Institute, Troy, New York, USA

Desmond Darby
Institute of Geological and Nuclear Sciences, Lower Hutt, New Zealand

Received 17 June 2004; revised 16 September 2004; accepted 30 September 2004; published 22 December 2004.

[1] The GPS velocity field in the North Island of New Zealand is dominated by the long-term tectonic rotation of the eastern North Island and elastic strain from stress buildup on the subduction zone thrust fault. We simultaneously invert GPS velocities, earthquake slip vectors, and geological fault slip rates in the North Island for the angular velocities of elastic crustal blocks and the spatially variable degree of coupling on faults separating the blocks. This approach allows us to estimate the distribution of interseismic coupling on the subduction zone interface beneath the North Island and the kinematics of the tectonic block rotations. In agreement with previous studies we find that the subduction zone interface beneath the southern North Island has a high slip rate deficit during the interseismic period, and the slip rate deficit decreases northward along the margin. Much of the North Island is rotating as several, distinct tectonic blocks (clockwise at 0.5–3.8 deg Myr^{-1}) about nearby axes relative to the Australian Plate. This rotation accommodates much of the margin-parallel component of motion between the Pacific and Australian plates. On the basis of our estimation of the block kinematics we suggest that rotation of the eastern North Island occurs because of the southward increasing thickness of the subducting Hikurangi Plateau. These results have implications for our understanding of convergent margin plate boundary zones around the world, particularly with regard to our knowledge of mechanisms for rapid tectonic block rotations at convergent margins and the role of block rotations in the slip partitioning process. *INDEX TERMS:* 1206 Geodesy and Gravity: Crustal movements—interplate (8155); 1243 Geodesy and Gravity: Space geodetic surveys; 8120 Tectonophysics: Dynamics of lithosphere and mantle—general; 8150 Tectonophysics: Plate boundary—general (3040); *KEYWORDS:* New Zealand, active tectonics, subduction, GPS, tectonic block rotation, slip partitioning

Citation: Wallace, L. M., J. Beavan, R. McCaffrey, and D. Darby (2004), Subduction zone coupling and tectonic block rotations in the North Island, New Zealand, *J. Geophys. Res.*, *109*, B12406, doi:10.1029/2004JB003241.

1. Introduction

[2] Geodetic studies from deforming zones often produce complex velocity fields, dominated by independent motion of tectonic blocks in addition to coupling on plate boundary faults [e.g., *McCaffrey et al.*, 2000a; *McClusky et al.*, 2001; *McCaffrey*, 2002; *Wallace et al.*, 2004]. To deal with this, an appropriate approach to the interpretation of geodetic data is to recall the fundamental plate tectonic assumption that the earth is composed of nondeforming tectonic blocks bounded by potentially coupled faults where the relative tectonic block motion is accommodated, and apply this notion to smaller-scale tectonic units. To implement this concept, some workers [e.g., *McCaffrey*, 1995; *Prawirodirdjo et al.*, 1997; *Meade and Hager*, 1999; *McCaffrey et al.*, 2000a; *McClusky et al.*, 2001; *McCaffrey*, 2002] have devised various methods for interpreting geodetic data in terms of elastic, rotating tectonic blocks, and interseismic coupling on faults between the blocks. This is a particularly important method to use at subduction zone margins, as the elastic effects from coupling on the subduction interface during the interseismic period can penetrate far inland, and tectonic blocks in these settings are often mobile, and separated from the upper plate by back-arc basins, strike-slip faults, and/or thrust belts.

[3] Sometimes, convergent plate boundary microblocks (CPBMs) rotate about nearby poles of rotation located within a few hundred kilometers of the microblocks (e.g., Cascadia, Marianas, Vanuatu, and Papua New Guinea)

0148-0227/04/2004JB003241$09.00

[*McCaffrey et al.*, 2000a; *Kato et al.*, 2003; *Calmant et al.*, 2003; *Wallace et al.*, 2004]. In cases where a CPBM rotates about a nearby axis at an obliquely convergent margin, Sumatra-style slip partitioning via upper plate strike-slip faulting can become largely unnecessary, as the margin-parallel component of relative plate motion can be accommodated by the block rotation [e.g., *McCaffrey et al.*, 2000a]. Where a CPBM (which often coincides with the forearc) rotates about a nearby axis, a combination of extension and contraction, rather than strike-slip occurs at the boundary between the rotating CPBM and the main part of the upper plate. This is quite different from the situation observed in Sumatra [*Fitch*, 1972] (widely considered to be the ''classic example'' of slip partitioning), where the relative rotation pole is far from Sumatra and most of the margin-parallel component of motion is accommodated by a single upper plate strike-slip fault. Accurate assessment of the kinematics of CPBMs may also help us discern the relative importance of the forces driving their rotation.

[4] Mapping the distribution and rate of strain accumulation at subduction zones is critical for understanding seismic hazards at these margins, as well as for gaining knowledge of what controls the location of seismogenic zones at subduction interfaces. GPS velocity fields in regions overlying a subduction zone are one of the primary sources of information about where interseismic coupling occurs on the subduction interface. Thus plate boundaries where land overlies part of the seismogenic portion of a subduction zone are important natural laboratories for studies of the seismogenic zone. Costa Rica, New Zealand, and Japan are good examples of such places.

[5] In this paper, we deal with two timescales of tectonic deformation in the North Island, New Zealand: (1) long-term tectonic rotation of the eastern North Island and (2) short-term (interseismic) elastic deformation due to coupling on faults, particularly the Hikurangi subduction zone. The North Island of New Zealand straddles the Australia/Pacific plate boundary, and is an example of an obliquely convergent margin whose interseismic velocity field is a result of block rotations and elastic strain [e.g., *Walcott*, 1984; *Beanland and Haines*, 1998; *Beavan and Haines*, 2001; *Darby and Beavan*, 2001]. Using geodetic, geological, and seismological data, we implement the elastic, rotating block approach explained by *McCaffrey* [1995, 2002] to estimate the angular velocities of the eastern North Island tectonic blocks, while simultaneously solving for the distribution of coupling on the Hikurangi subduction zone and other upper plate block-bounding faults. We show that rotation of the eastern North Island enables slip partitioning with less strike-slip faulting in the upper plate than would be expected from Sumatra-style partitioning. We also predict the rates of relative motion on some faults in the North Island region and suggest a possible mechanism for the rotation of the eastern North Island.

2. Tectonic Setting

[6] The North Island of New Zealand lies in the boundary zone between the obliquely converging Pacific and Australian plates. Australia-Pacific relative motion decreases in rate and takes on a greater margin-parallel component southward along the New Zealand margin [e.g., *DeMets et al.*, 1990, 1994] (Figure 1). Subduction of the thickened, oceanic Hikurangi Plateau occurs at the Hikurangi Trough east of the North Island (Figure 1). The Hikurangi Plateau changes northward to a normal oceanic plate subducting at the Kermadec Trench, the northern continuation of the Hikurangi Trough. In the South Island, subduction gives way to strike-slip dominated faulting, with the Marlborough Fault System and the Alpine fault accommodating most of Australia-Pacific relative motion [e.g., *Van Dissen and Yeats*, 1991; *Holt and Haines*, 1995; *Beavan et al.*, 1999; *Norris and Cooper*, 2000].

[7] North Island active tectonics is dominated by subduction at the Hikurangi Trough, back-arc rifting in the Taupo Volcanic Zone (TVZ), and strike-slip faulting in the eastern North Island dextral fault belt (NIDFB) (Figure 1). Extensive shortening in the accretionary wedge is observed between the Hikurangi Trough and the east coast of the North Island [*Barnes and Mercier de Lepinay*, 1997]. Upper plate shortening over the last 5 Myr also occurs in the subaerial portion of the eastern North Island, and is most prevalent south of 39 S [*Nicol et al.*, 2002; *Nicol and Beavan*, 2003; A. Nicol et al., Deformation within a plate boundary transition zone, Hikurangi subduction margin, New Zealand, submitted to *Tectonics*, 2004, hereinafter referred to as Nicol et al., submitted manuscript, 2004]. The TVZ (part of the Central Volcanic region, or CVR) has been opening for at least the last 2–4 Myr [*Stern*, 1987; *Cole et al.*, 1995], with estimated opening rates ranging from a few millimeters per year to 20 mm yr^{-1} (see *Villamor and Berryman* [2001] for summary). Rotation of the eastern North Island has been suggested from geological and geodetic results, and the extension and subaerial upper plate shortening in the North Island is presumably related to this rotation [e.g., *Walcott*, 1984; *Beanland and Haines*, 1998, *Beavan and Haines*, 2001; Nicol et al., submitted manuscript, 2004]. The dextral shear belt in the eastern North Island is estimated to accommodate ~20 mm yr^{-1} near 41°S, ~8 mm yr^{-1} near 40.5°S, and ~6 mm yr^{-1} of strike-slip motion in the north, near 38°S [*Beanland*, 1995; *Van Dissen and Berryman*, 1996], and has been active since at least 1 Ma [*Kelsey et al.*, 1995]. This observed slip is considerably less than 25 mm yr^{-1} near 38°S and 31 mm yr^{-1} near 41°S of margin-parallel Australia/Pacific relative motion that must be somehow accommodated across the North Island plate boundary zone. We suggest that block rotations can solve this ongoing dilemma.

3. GPS Data Analysis

[8] The GPS data we use are from 24 regional GPS deformation surveys conducted by the Institute of Geological and Nuclear Sciences between 1991 and 2003. These data are supplemented by two regional and five national GPS campaigns conducted for survey control by the Department of Survey and Land Information (now Land Information New Zealand) between 1994 and 1998. The surveys through 1999 were used by *Beavan and Haines* [2001] to calculate a continuous surface deformation model of New Zealand. In most of the regional surveys, effort has been made to both extend and densify the network as well as to reoccupy most or all of the previously surveyed stations. In each campaign, multiple

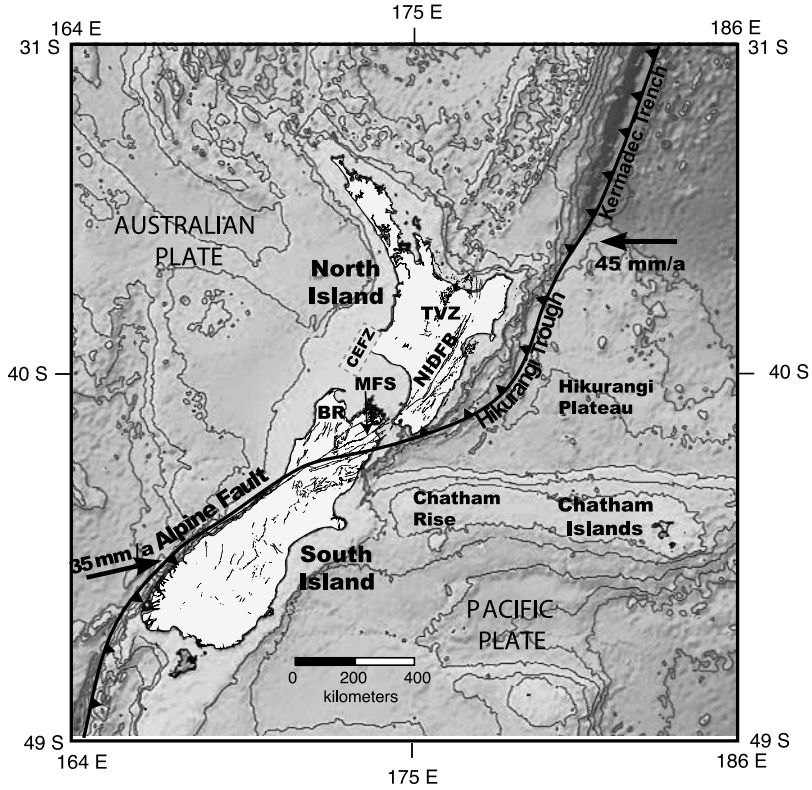

Figure 1. Regional tectonic setting of New Zealand. MFS, Marlborough Fault System; NIDFB, North Island Dextral Fault Belt; TVZ, Taupo Volcanic Zone; BR denotes approximate location of shortening-related faults of the Buller region in the northwestern South Island, and CEFZ indicates the region where extensional faulting occurs on the Cape Egmont Fault Zone. Arrows show Pacific/Australia relative motion in the New Zealand region [e.g., *DeMets et al.*, 1990, 1994]. See color version of this figure in the HTML.

sessions were observed where possible, with session lengths of 18–24 hours at most stations but as short as 7–8 hours in some cases. These shorter sessions occur mostly in the 1999 and earlier campaigns. The resulting network comprises about 350 stations distributed over the study region with the greatest density of GPS sites in the southern North Island (Figure 2). From a total of more than 5000 station days of data, about 3% of station observations are rejected because they appear as outliers (residuals greater than 3 standard errors) in single-survey variation of coordinate solutions. Some poorly determined station observations are rejected as a result of unusually short observing sessions (significantly less than 7 hours), and site velocities that are grossly inconsistent with neighboring stations are also removed.

3.1. Relative Coordinate Estimation

[9] The GPS phase data from all surveys were processed by standard methods using Bernese software versions 3.5 through 4.2. [*Rothacher and Mervart*, 1996; *Beutler et al.*, 2001] to determine daily estimates of relative coordinates and their covariance matrices during each survey. International GPS Service (IGS) elevation-dependent antenna phase center models [*Rothacher and Mader*, 1996] were used to account for the different antennas used. IGS final orbits and associated polar motion files were held fixed and one station's coordinates were tightly constrained during each day's processing. All but three campaigns were processed using orbits in modern versions of the International Terrestrial Reference Frame (ITRF): ITRF96, ITRF97 and ITRF2000. For the 1991 data from the central North Island, we used Scripps Institution of Oceanography (SIO) orbits and polar motion that have been reprocessed in ITRF2000 using modern software, rather than IGS orbits. For three early (1992, 1994, and 1995) southern North Island campaigns of limited spatial extent the data were processed in ITRF93. (Because of the way in which the data and solutions from these early campaigns were stored, it is nontrivial to repeat the solutions with modern software and orbits. However, we estimate that the maximum effect on our velocity solutions due to the use of the older orbits is at the submillimeters per year level, especially since most of the affected stations have been observed in several later surveys.) When combining the coordinate difference solutions from individual campaigns to generate velocity solutions we simultaneously solved for the local transformations between these frames, so that the resulting velocities are in the same reference frame (see section 3.2.1 below for more detail).

[10] For each survey, all daily coordinate difference solutions and their covariances were input to the least squares variation of coordinates software ADJCOORD [*Crook*, 1992] to check for outliers and to obtain the appropriate reduced χ^2 factor for subsequent scaling of the covariance matrix. The covariance matrices require

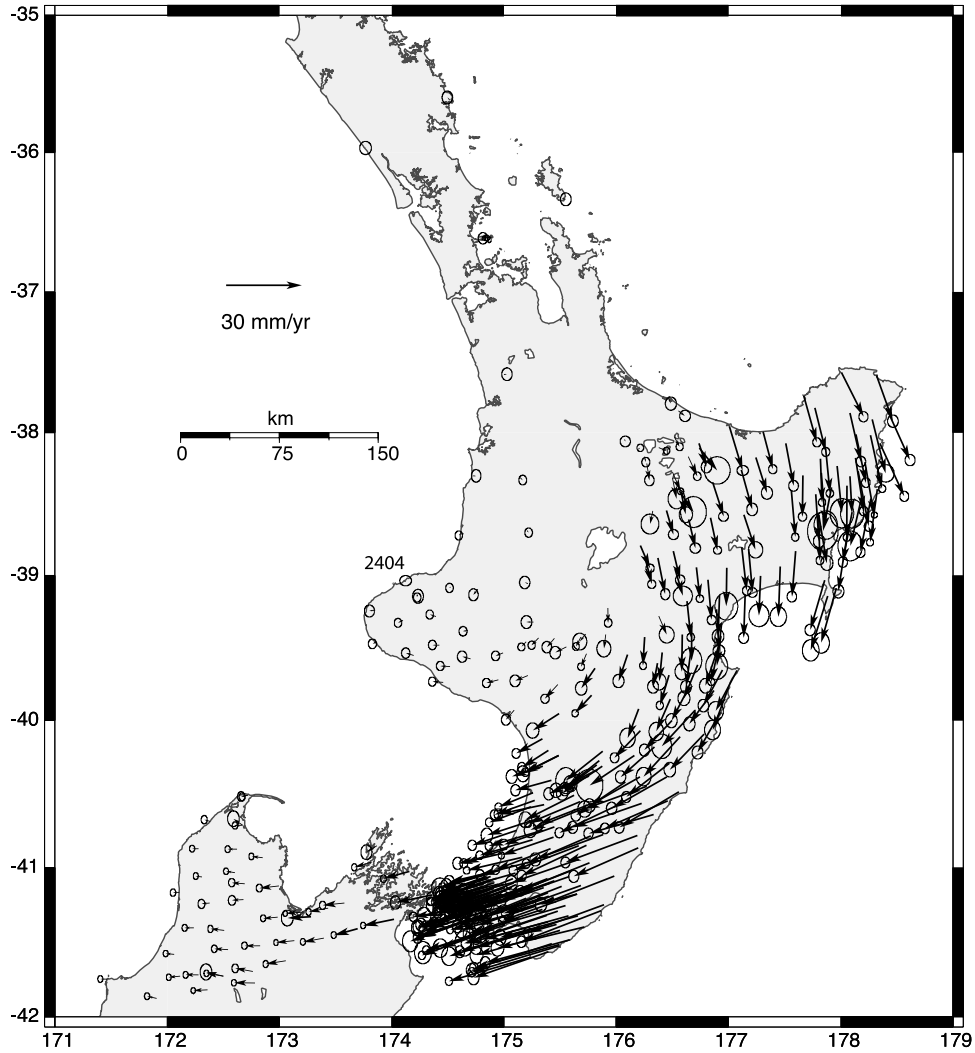

Figure 2. GPS velocity field in the North Island and northwestern South Island. All velocities are shown relative to the Australian Plate. Error ellipses are at 68% confidence level.

scaling because the temporal correlation of the GPS phase data is neglected in the estimation of the formal errors. The scaling factor depends on the noise properties of each data set, and also depends strongly on the sample interval of the GPS phase data used to obtain final coordinates. It varies from 4^2 to 8^2 for the 120-s samples we use in the final stages of our processing (30-s samples are used for data editing and cycle slip fixing, then the data are decimated to 120 s for subsequent processing). This procedure ensures that the relative coordinate uncertainties estimated from each survey are consistent with the scatter of repeated observations within that survey.

3.2. Velocity Estimation

[11] The daily coordinate differences and scaled covariance matrices for individual surveys are input to the ADJCOORD software to estimate station velocities and their uncertainties relative to a fixed station. ADJCOORD invokes the simultaneous estimation algorithm, where observations at different times are used for least squares estimation of deformation rate parameters simultaneously with the estimation of relative coordinates at some arbitrary time and the transformation parameters between different reference frames [*Bibby*, 1973, 1981, 1982]. The choice of fixed station is arbitrary, as the full coordinate difference covariances are propagated through the solution so that a transformation may always be made to any other fixed station.

[12] For largely historical reasons we combined the individual surveys into three separate velocity solutions: (1) the 1993–1998 nationwide surveys of about 30 stations; (2) all North Island campaign surveys from 1991 to 2003; and (3) northern South Island surveys of 1994–1996–1999. For the North Island solution, we chose station 2404 near New Plymouth as the fixed station (Figure 2) because it moves at close to Australian Plate velocity, and therefore the velocity field output from ADJCOORD is approximately in an Australian-fixed reference frame. The velocities will later be transformed to a precisely Australian-fixed frame as described in section 3.2.3. The other two solutions are treated similarly, but using different fixed stations. Some stations appear in more than one velocity solution. In these cases we retain all the separate velocity estimates, and these are

Table 1. Rotation and Uncertainties (σ) of the New Zealand GPS Data Sets Relative to the Australian Plate Reference Frame Defined in Our Modeling

	Rotation of GPS Data Sets[a]					
	ω_x	ω_y	ω_z	σ_x	σ_y	σ_z
Northern South Island (1994–1999)	0.084	−0.026	0.064	0.0045	0.0001	0.0032
NZ regional (first-order) network	0.019	−0.005	0.026	0.0056	0.0001	0.0034
Combined North Island campaigns	−0.011	−0.014	0.002	0.0002	0.0001	0.0001

[a]The rotation *x*, *y*, and *z* angular velocity components are in deg Myr^{-1}.

weighted according to their uncertainties in subsequent analysis.

3.2.1. Transformations Between Reference Frames

[13] Because we are using coordinate difference data, there are a maximum of four parameters, three rotations and a scale, to define the transformation between each reference frame. We solve for parameters that transform each of the ITRF93, ITRF97, and ITRF2000 coordinates into the ITRF96 frame. We choose local rotation axes, with one axis vertical near the centre of the network and two horizontal. The two rotations about horizontal axes depend almost entirely on vertical station coordinates for our network of about 600-km extent. These cannot be estimated accurately from the available vertical data and they have virtually no effect on the horizontal station velocities; we therefore set these parameters to zero. The scale parameters (i.e., the difference of the scale factor from unity) determined by the International Earth Rotation Service (IERS) between each of these ITRF realizations reaches a maximum of 1.4 ppb, or less than 1 mm across the entire extent of our network. Any velocity bias introduced by neglecting these scale parameters over the >10-year data duration is therefore no more than a few tenths of a millimeter per year. We attempted to estimate the scale factors between reference frames as part of our solution, but the areal extent of the network is too small to do this reliably. Because of these considerations, we have set the scale parameters of all our reference frames to zero. This leaves just the vertical rotation parameter, Ω, which is the one that has the largest potential effect on the horizontal velocities estimated in a network of limited areal extent. Our solutions for Ω are $\Omega_{ITRF93\rightarrow ITRF96} = -0.007 \pm 0.003$ μrad, $\Omega_{ITRF97\rightarrow ITRF96} = 0.000 \pm 0.001$ μrad, and $\Omega_{ITRF2000\rightarrow ITRF96} = 0.000 \pm 0.001$ μrad. Therefore it is only the three southern North Island coordinate difference solutions that used ITRF93 orbits that are modified by the changes in reference frame realization.

3.2.2. Reference Frame of Resulting Velocity Field

[14] The resulting relative velocities have taken account of the differences in orientation between the various ITRF realizations. However, because the velocity of the chosen fixed station is zero, these velocities are not actually in the ITRF96 reference frame. However, the velocities are aligned with ITRF96 in the sense that if the velocity field is rotated about a pole to the location of the fixed station so as to give that station its ITRF96 velocity, then all the other stations will also have ITRF96 velocities.

3.2.3. Transformation to Australia-Fixed Frame

[15] We now transform the relative velocities from their alignment with the ITRF96 reference frame to a frame fixed with respect to the Australian Plate. We do this by inputting the three velocity fields into the velocity modeling software of *Beavan and Haines* [2001]. One output of this software is the Euler vector that transforms each input velocity data set into a best fit to an Australia-fixed reference frame, using an assumption that the model boundary some 50 km off the west coast of New Zealand is a part of the rigid Australian Plate. Because this is an assumption that can be challenged, the Euler rotation between each velocity data set and the rigid Australian Plate is left as an optional free parameter when interpreting the combined velocity field in terms of block rotations and elastic strain (see section 4 and Table 1).

3.3. Velocity Uncertainties

[16] ADJCOORD assumes a white noise model when estimating velocity uncertainties. However, the velocity uncertainty estimates are scaled by $\sqrt{(\chi\nu^2)}$ of the fit of the uniform velocity solution to the relative coordinate data. This factor varies between 1.0 and 1.5 for our three velocity solutions. This weighting provides a partial allowance for the colored noise that is expected to be present in GPS coordinate time series due to temporal correlations in the data [e.g., *Zhang et al.*, 1997]. It should be noted that we are analyzing relative coordinate time series within a network of limited (∼600 km) extent. The magnitude of colored noise present in such time series is significantly smaller than the effects seen in time series from global or regional networks where the coordinates are placed in a global reference frame such as ITRF96 prior to velocity estimation [e.g., *Williams et al.*, 2004]. This is because colored noise from the orbits, reference frame and other causes are propagated into each velocity time series in the latter case. In our case, these effects are diminished because they are essentially common mode across the network. Nevertheless, we expect that our velocity uncertainties remain underestimated due to residual effects of colored noise (e.g., tropospheric noise) and to station reoccupation noise that has not been fully characterized by the procedures discussed above. For example, the velocity uncertainty at a station occupied in only two campaigns contains no contribution from reoccupation noise. *Beavan and Haines* [2001] found that an additional factor of about 1.5 was required when fitting New Zealand GPS campaign velocity solutions to a smooth, continuous velocity field. We scale our velocity uncertainties in the following analysis (section 4) by a similar factor.

4. Data Modeling Approach

[17] To interpret the GPS velocity field in the North Island (Figure 2), we employ an inversion approach that simultaneously estimates the angular velocities of elastic blocks on a sphere, and slip fractions (e.g., coupling coefficients) on block-bounding faults, to give the best possible fit to the GPS velocities, and optionally to earthquake slip vectors and geologic fault slip rate estimates

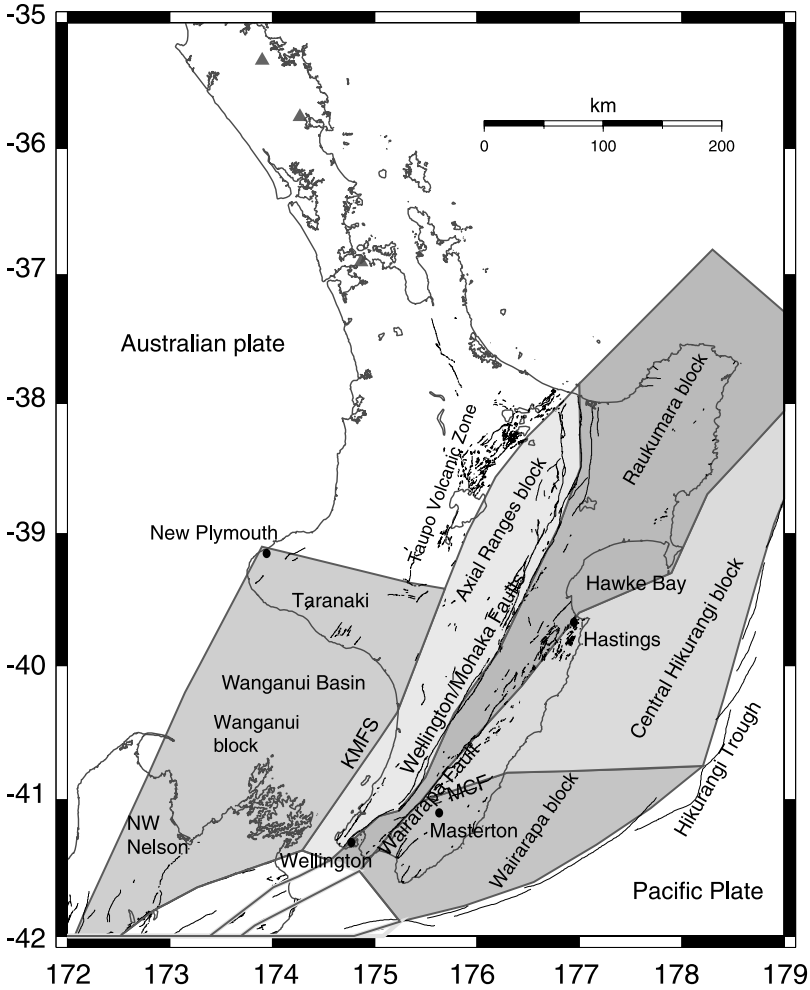

Figure 3. Tectonic block configuration described in this paper. Surface traces of known active faults (from Institute of Geological and Nuclear Sciences' active fault database) are also shown, and some are labeled. MCF, Masterton and Carterton Faults; KMFS, Kapiti Manawatu Fault System. The locations of Wellington, Hastings, Masterton, and New Plymouth are noted. See color version of this figure in the HTML.

[*McCaffrey*, 1995, 2002]. This method applies simulated annealing to downhill simplex minimization [e.g., *Press et al.*, 1989] to solve for the angular velocity vectors of specified tectonic blocks and slip fractions for faults between the blocks. We minimize data misfit, defined by the reduced chi-squared statistic (χ^2_n). The method also allows us to optimally rotate GPS velocity solutions from different data sets into a common reference frame. In our case, we estimate a rotation of the three New Zealand GPS velocity solutions (discussed in section 3.2) into an Australian Plate reference frame.

[18] We specify several tectonic blocks in the North Island, basing our block boundaries not on the GPS data, but on geological and seismological evidence for active faulting (Figures 3 and 4). There is evidence for very slow deformation on faults contained within some of the tectonic blocks we define, but the rates of motion on faults in the blocks interiors are typically an order of magnitude lower than the motion on the block bounding faults [e.g., *Nicol et al.*, 2002]; deformation associated with the more slowly slipping block interior faults is unlikely to be detectable within the uncertainties of GPS measurements. For the purposes of this paper, we address only the North Island and northwestern South Island. We use *F* tests on the distributions of residuals to assess whether particular tectonic blocks are required by the GPS data (see section 6.1). We define two eastern tectonic blocks (the Wairarapa and Central Hikurangi blocks) between the Hikurangi Trough and the Wairarapa fault, and related faults continuing north of the Wairarapa fault. The boundary between the Central Hikurangi and Wairarapa blocks is defined by the Masterton and Carterton faults (Figure 3). In the initial stages of the modeling, we treated the Central Hikurangi and Wairarapa blocks as a single composite block; we discuss in section 6.5 the reasons for dividing the Central Hikurangi and Wairarapa blocks into two separate blocks. We specify a Raukumara block between the Wellington/Mohaka and Wairarapa faults, encompassing most of the northeastern North Island. We include a block bounded by the Wellington/Mohaka faults to the east, and the TVZ and Kapiti-Manawatu Fault System (KMFS) to the west (Axial Ranges block). We also solve for the rotation of an independent block to the west of the Axial Ranges block, encompassing much of Taranaki

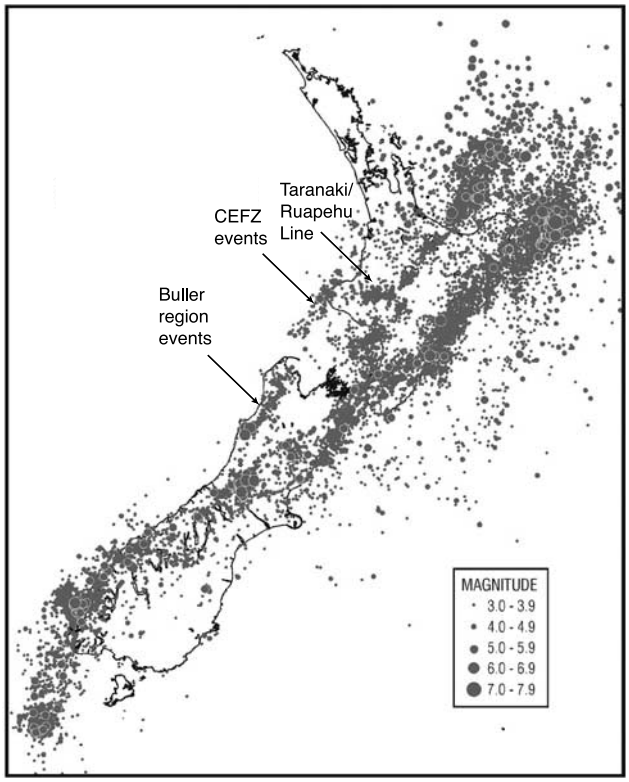

Figure 4. Shallow seismicity from 1990 to 1999, depths <40 km. Source is: Institute of Geological and Nuclear Sciences. CEFZ, Cape Egmont Fault Zone. See color version of this figure in the HTML.

and the northwestern South Island (the Wanganui block). The northern boundary of the Wanganui block is defined by a linear, shallow seismic zone extending from the southern end of the TVZ toward Mt. Taranaki (the Taranaki/Ruapehu line) [e.g., *Reyners*, 1980, 1989], and the western boundary is defined by a north-northeast trending seismic zone off the west coast of the North Island, extending southward into the northwestern South Island [*Anderson and Webb*, 1994] (Figures 3 and 4). Note that we have removed the GPS data in the Taupo Volcanic Zone (TVZ) region from the inversion, due to the complex tectonic and volcanic deformation there. However, we can use our estimate of relative motion between the Axial Ranges block and the Australian Plate to constrain the total rate of rifting in the TVZ.

[19] The short-term (interseismic) slip rate close to and across most faults is considerably less than the long-term slip rate expected from the relative motion of the adjacent tectonic blocks. This phenomenon, which is caused by the friction between the two sides of the fault, is often referred to as "locking" or "coupling" and gives rise to elastic strain rates in the rocks adjacent to the fault. There exists some confusion regarding how to describe this feature of faults and what it means [*Wang and Dixon*, 2004; *Lay and Schwartz*, 2004]. For our purposes we refer to a purely kinematic quantity we call the "slip rate fraction," ϕ. If V is the long-term slip rate on the fault (over many earthquake cycles) and V_c the short-term creep rate (the steady displacement rate across the fault surface over a short time), then $\phi = 1 - V_c/V$. If $\phi = 0$, the fault is creeping at the full long-term slip rate, and if $\phi = 1$, there is no creep in the interseismic period. We represent fault slip behavior as somewhere between those two extremes. In the case where ϕ is neither 0 nor 1, one could interpret it as a spatial average of creeping and noncreeping patches [*Scholz*, 1990; *McCaffrey et al.*, 2000a, 2000b; *Lay and Schwartz*, 2004].

[20] We solve for the distributions of the "slip rate fraction," ϕ, on the Hikurangi subduction zone, the North Island Dextral Fault Belt, Masterton/Carterton, Wairarapa, KMFS, and TVZ boundary faults (Figure 1). We use fault parameters and fault surface traces compiled by *Stirling et al.* [2002] to define most of the block-bounding faults (other than the subduction zone). We use the Hikurangi subduction zone geometry determined by *Ansell and Bannister* [1996] to define the subduction zone thrust fault in the modeling. We specify individual nodes on the subduction zone, spaced on average 30 km apart along strike, and at depths of 5, 10, 15, 20, 25, 35, and 50 km (Figure 5), and solve for ϕ at each of them. To represent the linear change in ϕ values between adjacent nodes, values on small rectangular fault patches between the nodes are estimated by bilinear interpolation. These fault patches are 3 km long in the strike-parallel direction, and 3 km wide in the downdip direction. We impose an along-strike smoothing constraint on the ϕ values by keeping their along-strike change below a specified value. For example, a smoothing constraint of 0.5 permits a variation in ϕ of 0.5 or less over a 1° distance (~111 km) along strike, while a very low smoothing value (<0.1) will produce an extremely smooth model. We estimate that the optimum smoothing parameter to use in the New Zealand case is 0.5 based on the fact that values higher than this (allowing large variations in ϕ over wavelengths shorter than ~50 km, or 0.5°), do not yield a significant improvement in fit to the data.

[21] The relative motion on the faults is determined by the Euler vector describing the motion of the blocks on either side of the fault. The slip rate deficit vector on the fault is the scalar coupling value ϕ multiplied by the relative motion vector V between the two blocks at a given fault patch. The elastic contribution to the velocity field from the fault slip rate deficit is calculated using a back-slip approach to elastic dislocation modeling [*Savage*, 1983], using the formulations of *Okada* [1985] for surface displacements due to dislocations in an elastic, half-space. For further details on how block bounding faults are dealt with in this paper, we refer the reader to *McCaffrey* [2002].

[22] We also impose the constraint that ϕ on the faults decreases downdip from a value of one (full interseismic coupling) at the surface. This is appropriate for terrestrial faults in New Zealand as no evidence exists for aseismic surface creep on any of these faults. The downdip constraint is necessary when using an elastic dislocation modeling approach at a subduction interface in order to avoid the unrealistic extensional strain above the updip end of the coupled zone that is predicted by the model when the area updip of the coupled zone of a dipping fault slips aseismically [e.g., *McCaffrey*, 2002]. This means that we cannot discern the actual updip end of coupling on the subduction interface using elastic dislocation methods.

4.1. Resolution Tests

[23] We conducted a "zebra test" to determine at what wavelengths, and how far offshore our GPS network can

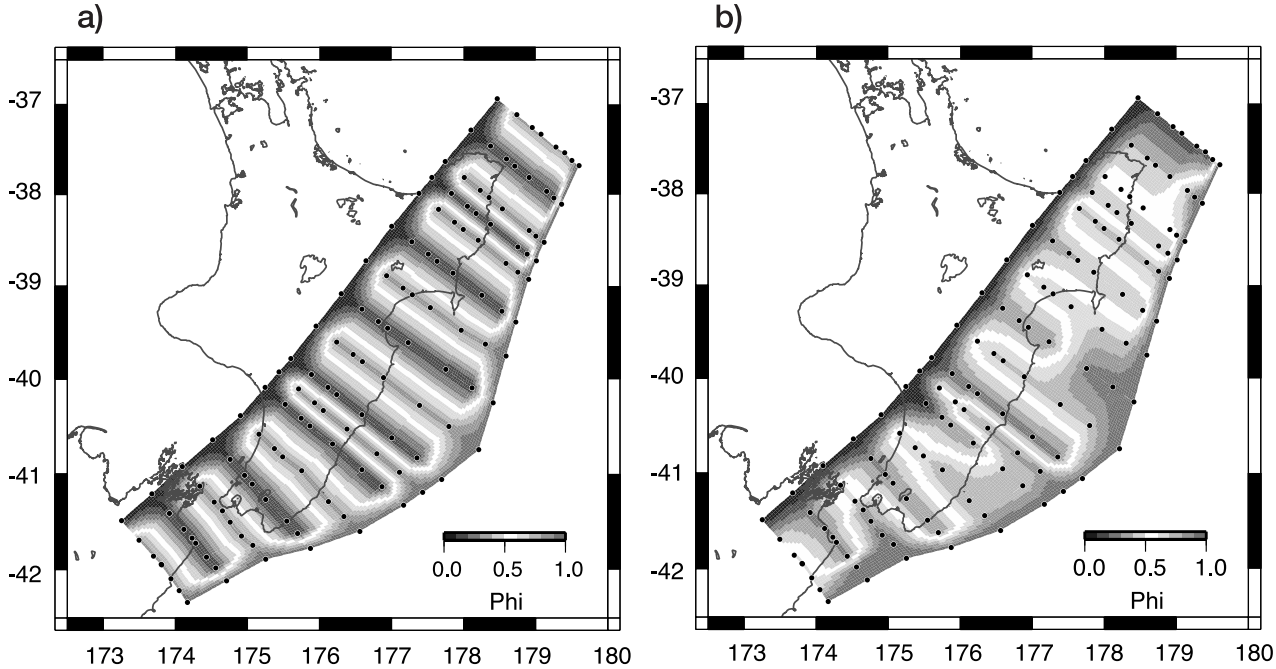

Figure 5. Results of resolution test for locking on the Hikurangi subduction interface. (a) Assumed locking distribution for the forward model; (b) locking distribution recovered by inversion of the "noisy" data generated by the forward model. Phi (ϕ) refers to the degree of coupling. A ϕ value of 1.0 corresponds to full interseismic coupling, and 0 means no coupling (aseismic creep). See color version of this figure in the HTML.

resolve variations in slip rate deficit (Figure 5). To do this, we calculate the predicted GPS velocities at all of our sites for a ϕ distribution identical to that in Figure 5a. We add white noise characteristic of the estimated uncertainties to the predicted velocities, and then invert these data to estimate the ϕ distribution from the "noisy" data. The inversion (Figure 5b) shows if our ϕ values change markedly along strike over a distance of 50 km, that our GPS network would detect this. It is also clear from the zebra test that the ϕ estimates are less well resolved for the offshore regions. This is expected given that GPS observations are restricted to land.

4.2. Other Data Used in the Inversion

[24] In addition to the New Zealand GPS data discussed in the previous section, we also use GPS velocities on the Pacific and Australian plates from *Beavan et al.* [2002]. The *Beavan et al.* [2002] velocities help us to more solidly establish an Australian Plate reference frame, as well as providing a Pacific plate boundary condition for the kinematic modeling. We use earthquake slip vector azimuths from *Webb and Anderson* [1998], *Doser et al.* [1999], and *Doser and Webb* [2003] on faults in the region. We include long-term fault slip rate information (e.g., 1–20 kyr or longer, largely from paleoseismological studies) from upper plate faults in the southern North Island (most notably the Wellington and Wairarapa faults) [*Berryman*, 1990; *Van Dissen et al.*, 1992; *Beanland*, 1995; *Van Dissen and Berryman*, 1996; *Beanland and Haines*, 1998; *Kelsey et al.*, 1998; *Grapes*, 1999]. In some cases, we also impose constraints that relative motion across a block boundary should occur in a range of directions consistent with geological observations. For example, where shortening is observed on Quaternary faults on the eastern boundary of the Wanganui block [e.g., *Melhuish et al.*, 1996; *Jackson et al.*, 1998; *LaMarche et al.*, 2003], we impose the constraint that the relative motion across that boundary should fall within a range of azimuths consistent with shortening. In some cases, the slip rate and slip azimuth information are treated as data, with realistic uncertainties (i.e., having a normal distribution), while in other cases we treat the data as a "hard constraint," where a penalty function is imposed if the model relative motion direction and rates fall outside of the appropriate range of values (these data have a uniform distribution). All slip azimuth and slip rate data used and, whether they are treated as data or as a hard constraint, are summarized in Table 2.

5. Results From the Best Fitting Model

[25] In our best fitting model, we obtain $\chi^2 = 1.32$ (736 observations, 598 degrees of freedom (DOF)) (Figure 6). We estimate the angular velocities of five tectonic blocks, parameters for the rotation of three GPS data sets into an Australian Plate reference frame, and ϕ values at 114 nodes on faults bounding the blocks. The poles of rotation we obtain for the various blocks, and the rotation parameters for the New Zealand GPS data sets are shown in Table 3 and Figure 7. As nearly all of our Australian and Pacific plate site velocities are from *Beavan et al.* [2002], our Australia/Pacific Euler pole is identical to theirs. For the New Zealand data sets, we find (Table 1) that the rotations between the nominally Australian-fixed input velocity field and the Australia-fixed velocity field obtained in the inversion are very small. They

Table 2. Slip Vector and Fault Slip Rate Data Used in the Inversion

Block Pairs[a]	Data Type[b]	HC?[c] (Y/N)	Latitude	Longitude	Data Used	Modeled Value	Source[d]
PACI-CHKG	EQ SV	N	178.80	−38.85	315 ± 10	294	DW2003
PACI-CHKG	EQ SV	N	178.87	−38.42	310 ± 10	293	DW2003
PACI-CHKG	EQ SV	N	176.62	−40.30	298 ± 10	285	WA1998
PACI-CHKG	EQ SV	N	176.31	−40.51	298 ± 10	283	WA1998
PACI-RAUK	EQ SV	N	176.25	−39.74	280 ± 10	278	WA1998
PACI-RAUK	EQ SV	N	177.91	−38.45	295 ± 12	286	WA1998
PACI-WAIR	EQ SV	N	175.29	−41.51	279 ± 10	281	WA1998
PACI-WAIR	EQ SV	N	176.11	−41.51	284 ± 10	294	DW2003
RAUK-AXIR	GSR	Y	175.17	−41.12	5.0–7.8	6.9	BE1990
RAUK-AXIR	GSR	Y	174.72	−41.33	4.0–7.0	6.9	VD1992
WAIR-RAUK	GSR	Y	175.12	−41.33	8.0–11.0	8.0	G1999, and BH1998
CHKG-RAUK	GSR	Y	175.92	−40.56	1.1–4.1	2.2	BH1998
CHKG-RAUK	GSR	Y	176.7	−39.8	0.4–2.8	2.2	K1998
CHKG-WAIR	GSR	Y	175.9	−40.9	0.5–5.5	5.3	Z2000
CHKG-WAIR	GSR	Y	176.3	−40.8	0.5–5.5	5.4	Z2000
RAUK-CHKG	AZI EST	Y	175.6	−40.8	40–80	61	BHK
RAUK-CHKG	AZI EST	Y	176.23	−40.35	50–90	57	BHK
RAUK-CHKG	AZI EST	Y	176.73	−39.7	50–120	50	BHK
RAUK-WAIR	AZI EST	Y	174.72	−41.33	50–80	75	SSWAIR
WANG-AUST	EQ SV	Y	173.63	−39.65	159–179	165	WA1998
WANG-AUST	EQ SV	Y	172.29	−41.65	255–320	275	DW1999
WANG-AUST	EQ SV	Y	171.96	−41.76	301–281	282	DW1999
RAUK-AXIR	AZI EST	Y	174.72	−41.13	25–60	26	WELLF
RAUK-AXIR	AZI EST	Y	177	−38	340–030	22	WELLF
WANG-AXIR	AZI EST	Y	175.2	−40.35	40–140	40	KMFEST
WANG-AXIR	GSR	Y	175.2	−40.35	0.4–2.5	2.5	KMFEST
WANG-AXIR	AZI EST	Y	175.0	−40.7	40–140	71	KMFEST
WANG-AXIR	GSR	Y	175.0	−40.7	0.5–3.5	3.4	KMFEST

[a]AUST, Australia; PACI, Pacific; CHKG, Central Hikurangi block; RAUK, Raukumara block; AXIR, Axial Ranges block; WAIR, Wairarapa block; WANG, Wanganui block.

[b]EQ SV, earthquake slip vector; GSR, geological slip rate; AZI EST, possible range of sense of motion across a fault system/block boundary. All GSR data shown are in mm yr^{-1}, and all EQ SV and AZI EST are shown in degrees east of north for the first block relative to the second block.

[c]HC, treated as a hard constraint using a penalty function (data assumed to have a uniform distribution).

[d]DW2003, *Doser and Webb* [2003]; WA1998, *Webb and Anderson* [1998]; BE1990, *Berryman* [1990]; VD1992, *Van Dissen et al.* [1992]; G1999, *Grapes* [1999]; BH1998, *Beanland and Haines* [1998]; K1998, *Kelsey et al.* [1998] (we double their maximum estimate of 1.4 mm yr^{-1}, as they acknowledged there are likely to be other active faults in the area which may double the total fault slip rate estimate there); Z2000, *Zachariasen et al.* [2000] (note that slip rate estimates on the Carterton and Masterton faults are not well determined, so we put a reasonably large range which cover the possible rate of 2–4 mm yr^{-1} suggested by Z2000); BHK, a range of possible fault slip azimuths combining general observations from K1998 and BH1998 concerning the degree of shortening and strike slip on the faults continuing northeast of the Wairarapa Fault System (north of ~41°S); SSWAIR, a range of fault slip azimuths consistent with the general consensus in the literature that the Wairapa fault is dominantly strike slip, possibly with a component of shortening; DW1999, *Doser et al.* [1999], we use an average range of their multiple estimates for earthquake slip vectors in the Buller region; WELLF, range of azimuths taking into consideration the rough orientation of Wellington and Mohaka faults, plus the knowledge (from BE1990, VD1992, among others) that it is dominantly right-lateral strike slip; KMFEST, rough estimates derived from observations by *Melhuish et al.* [1996], *Jackson et al.* [1998], and *LaMarche et al.* [2003] of slow shortening on the Kapiti-Manawatu Fault System and strike-slip on the Ohariu Fault [*Heron et al.*, 1998].

amount to velocity changes of <0.5 mm yr^{-1} across the full extent of the network. Table 2 shows the fit to the geological slip rate and earthquake slip vector data. From the residuals of the observed GPS velocities to the best fitting model (Figure 6), we estimate the residual strain for each block (Table 4). Significant amounts of residual strain may indicate a systematically imperfect fit of the model to the data, or deformation (possibly on faults) within the blocks.

6. Discussion

6.1. Statistical Tests of Alternative Fault Coupling and Block Configuration Scenarios

[26] To test whether or not GPS velocities in the North Island can be explained solely by coupling on the subduction interface, or likewise by block rotations alone, we solved for situations where only coupling on the subduction interface is allowed, or only block rotations are allowed. In the case where block rotations only were considered, we obtain χ^2 = 3.8 (736 observations, 712 DOF). In the case where all of the North Island was assumed to be part of the Australian Plate (i.e., no block rotations), and fault coupling on the subduction zone alone was considered, χ^2 = 10.7 (728 observations, 617 DOF). The better fit obtained when inverting only for tectonic block rotations (compared to the consideration of fault coupling only) indicates that the GPS velocities in the North Island are largely a product of block rotations. However, solving for block rotations and fault coupling simultaneously gives the best fit to available data in the North Island (χ^2 = 1.32). Solving for block rotations and fault coupling satisfies the *F* test extremely well (Table 5), with an insignificant probability that the improvement in fit by including both fault coupling and block rotations in the model is purely due to chance.

[27] The projection to the Earth's surface of the angular velocity vectors (i.e., poles of rotation) that we estimate for each block occur quite close to one another (Figure 7 and Table 3), meaning that the angular velocities are nearly parallel to one another. The rates of rotation of these blocks relative to the Australian Plate range from 0.5 to 3.8 deg Myr^{-1} (clockwise). Although we determine the block configuration based on seismological and geological evidence, we have conducted *F* tests to determine whether

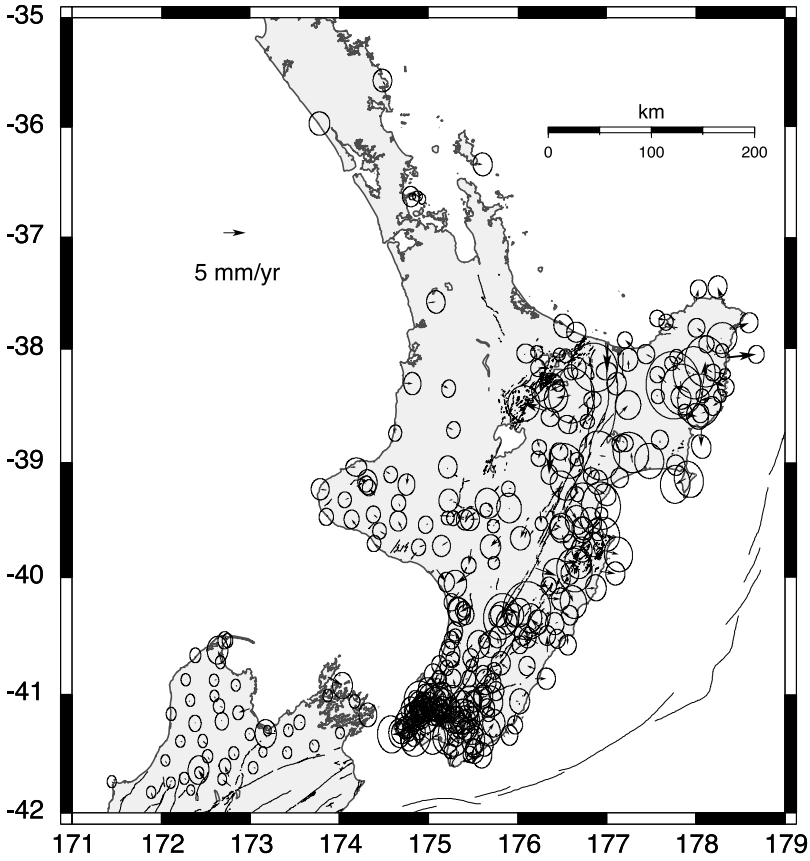

Figure 6. GPS velocity residuals for best fitting block rotation/fault locking model (with 68% confidence ellipses).

or not the GPS velocities require these blocks to be independent of one another (Table 5). For these tests we use only the GPS velocities and earthquake slip vectors on the subduction interface.

[28] From these tests, we conclude that the Wanganui block is distinct from the other North Island blocks (and the Australian Plate) by comparing models 4, 5, and 6 in Table 5. Comparing models 7 and 8 with model 6 (Table 5) shows that the GPS data require the easternmost tectonic blocks to be somehow divided in separate slivers. However, the GPS data on its own cannot be used to determine the details of how the Wairarapa, Axial Ranges block, Central Hikurangi, and Raukumara blocks should be divided into separate entities (compare model 1 with models 7 and 8, Table 5). The inconclusive *F* test result regarding the detailed division of the easternmost blocks (when using the GPS data only) highlights the importance of accounting for geological and seismological data in this type of modeling. If we used only GPS data in the block modeling, we would have come to the conclusion that the eastern North Island is composed of one or two tectonic blocks (plus an independent Wanganui block). However, the extensive seismological and geological evidence for active faulting on the Wellington/Mohaka faults, Wairarapa fault, and other upper plate faults in the North Island show that this is not the case. Given that the geodetic data fit both possibilities equally well, we prefer the interpretation that the eastern North Island is broken up into multiple slivers, as this is more consistent with the geological and seismological evidence. Care must be taken when interpreting geodetic data in complex tectonic settings, as it may be possible to fit GPS velocities with a variety of kinematic and fault slip rate deficit scenarios. Scenarios which fit the geodetic data, but violate other types of data (e.g., seismological and geological data) should be considered invalid, particularly if scenarios can be found that agree with all of the available data types.

6.2. Subduction Zone Slip Rate Deficit Estimates

[29] Previous workers infer that there is a variation in the degree of interseismic slip rate deficit on the subduction

Table 3. Euler Vectors for the Tectonic Blocks Discussed in This Study Relative to the Australian and Pacific Plates[a]

Plate Pairs	Longitude	Latitude	Rate, deg Myr^{-1}	e_{max}	e_{min}	Azimuth
AUST/RAUK	172.88	−39.44	−2.84 ± 0.37	0.53	0.29	314
AUST/WAIR	172.99	−38.86	−3.76 ± 2.25	2.69	0.45	304
AUST/WANG	172.49	−39.87	−0.44 ± 0.02	0.32	0.29	237
AUST/AXIR	173.33	−39.98	−2.8 ± 0.40	0.24	0.20	211
AUST/CHKG	172.78	−39.15	−2.99 ± 0.41	0.8	0.34	308
PACI/RAUK	175.05	−45.43	−3.85 ± 0.37	0.66	0.15	265
PACI/WAIR	174.68	−43.82	−4.77 ± 2.25	1.78	0.25	259
PACI/WANG	179.59	−55.08	−1.5 ± 0.02	0.22	0.07	305
PACI/AXIR	176.26	−45.86	−3.82 ± 0.4	0.89	0.13	277
PACI/CHKG	174.87	−45.00	−4.0 ± 0.41	0.63	0.22	261

[a]In all cases, Euler vectors are for the second plate relative to the first; e_{max}, e_{min}, and azimuth refer to the maximum and minimum uncertainties of the error ellipse (in deg) and the azimuth of the major axis, respectively. Negative rotation rates indicate clockwise motion. See Figure 10 caption for key to block name abbreviations.

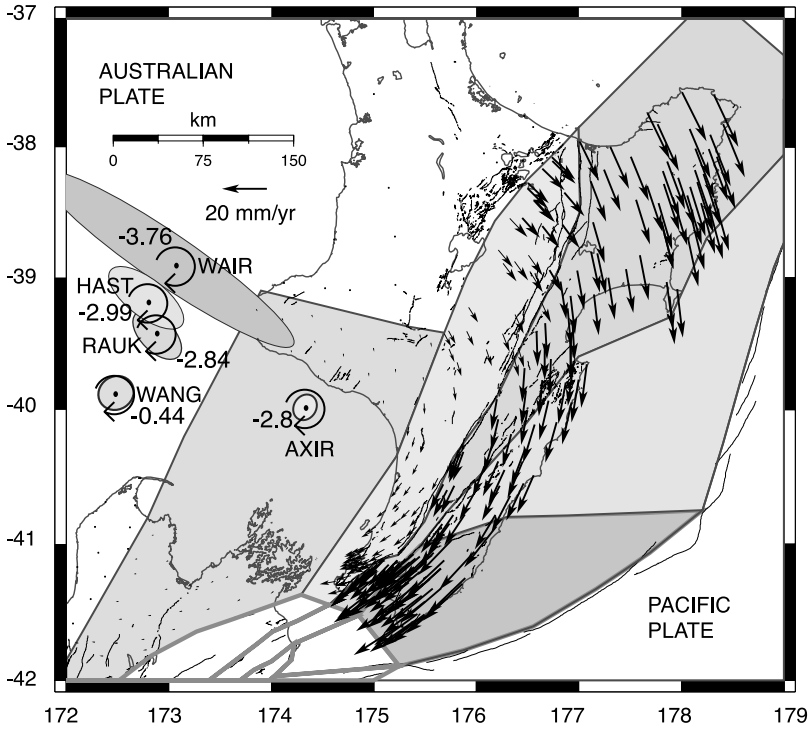

Figure 7. GPS site velocities predicted by long-term block rotations (i.e., short-term, elastic part removed). Locations and uncertainty ellipses of poles of rotation for each tectonic block relative to the Australian plate are also shown. Rotation rates (in deg Myr^{-1}) are shown next to the error ellipses (negative indicates clockwise rotation). The block that each pole corresponds to is denoted by the four-letter code next to the pole (Table 2 caption has key to block name codes). See color version of this figure in the HTML.

zone along the Hikurangi margin, progressing from a low slip rate deficit in the northern part of the margin to a high slip rate deficit in the southern part [*Walcott*, 1984; *Reyners*, 1998]. *Darby and Beavan* [2001] used geodetic data to infer that the subduction interface beneath the southern North Island has a ϕ value close to 1.0 during the present interseismic period. Our results are consistent with these observations, showing a high slip rate deficit beneath most of the lower North Island at present, and decreased slip rate deficit northward along the margin (Figure 8). Because of the presence of distinct tectonic blocks, the slip rate deficit on the subduction interface is not directly related to Pacific/Australia relative motion, but depends on the rates of motion between the upper plate blocks and the subducting Pacific plate. This study is the first time that the slip rate deficit on the Hikurangi subduction zone has been directly estimated, and these results are important for seismic hazard assessment in the North Island. Eventually the accumulated slip deficit will be released in an earthquake or a slow, aseismic slip event on the fault. The contribution from the interseismic fault slip deficit to the GPS site velocities is shown in Figure 9.

[30] In the southern North Island the yearly slip deficit on the subduction interface ranges from 20 to 30 mm yr^{-1}, with a slip deficit of ~20 mm yr^{-1} beneath the Wellington region. Northeast of the southern North Island, the slip rate deficit decreases (Figure 8). *Reyners* [1998] suggests a moderate degree of seismic coupling in the Hawke's Bay region from seismological evidence. Thus it is likely that some coupling on the Hikurangi subduction zone occurs beneath Hawke Bay (where there is no GPS data available), but we suggest from the GPS results that the coupled portion of the subduction zone in the Hawke's Bay region does not project onshore significantly. We discern a small patch of moderate coupling (slip deficit of 10–15 mm yr^{-1}) beneath the Raukumara Peninsula northeast of Gisborne (Figure 8), projecting onshore directly beneath an area of documented high (4 mm yr^{-1}) coastal uplift [*Ota et al.*, 1988,1992]. Numerous seamounts enter the subduction zone in the Raukumara Peninsula region [e.g., *Collot et al.*, 1996, 2001], and these features could be acting as asperities, causing the elevated slip rate deficit we observe from the geodetic data. Note that we constrained the ϕ value on the subduction interface to be 1.0 between 0 and 5 km

Table 4. Block Residual Principal Strain Rate Estimates and 1σ Uncertainties[a]

Block[b]	ε_1	ε_2	Azimuth ε_1[c]
RAUK	−5.2 ± 4.3	24.7 ± 5	16 ± 6.5
WAIR	−15.2 ± 13.8	34.7 ± 11.8	26 ± 10
WANG	−0.8 ± 3.1	10.5 ± 3.0	260 ± 15
AXIR	−10.7 ± 5.7	−9.2 ± 6	322 ± 33
CHKG	12 ± 18.4	18.25 ± 18	6 ± 27

[a]In units of 10^{-9} yr^{-1}. These strain rates are estimated from the residual of the best fitting model to the GPS observations. Negative numbers signify contraction.
[b]See the caption for Figure 10 for the key to block name abbreviations.
[c]Azimuth is in degrees east of north.

Table 5. Results of *F* Tests for Block Independence[a]

Model	N_{data}	$N_{parameters}$	DOF	χ^2_n	Number of North Island Blocks
1, best model	736	138	598	1.32	5
2, no rotation[b]	728	111	617	10.7	0
3, no coupling[b]	736	24	712	3.8	5
4, one block[c]	736	122	614	2.7	1
5, WANG = AUST[d]	736	118	618	1.72	1
6, WANG free[e]	736	125	611	1.60	2
7, model A[f]	736	131	605	1.37	3
8, model B[f]	736	135	601	1.35	4

Comparison of Models	Probability	Result
Is model 1 better than model 2?	0.99	yes
Is model 1 better than model 3?	0.99	yes
Is model 5 better than model 4?	0.99	yes
Is model 6 better than model 4?	0.99	yes
Is model 7 better than model 6?	0.97	yes
Is model 8 better than model 6?	0.98	yes
Is model 1 better than model 7?	0.68	maybe
Is model 1 better than model 8?	0.61	maybe

[a]*F* test results for various tectonic block/fault coupling models. We use all GPS, slip rate, and slip vector data (Table 2) for model 1, GPS data only for model 2, and GPS data and slip vectors on the Hikurangi subduction zone for models 3–8. See Figure 10 caption for block name abbreviations. DOF, degrees of freedom.

[b]The "no coupling" model refers to the situation where block rotations only are allowed; likewise, "no rotations" refers to a model where only fault coupling on the subduction zone is used to try to fit the data (i.e., the entire North Island is assumed to be part of Australia).

[c]The "one block" model is where all the eastern North Island blocks (including the Wanganui block) are considered to rotate as a single, large block.

[d]This model is where the Wanganui block is as assumed to be part of Australia, and the rest of the blocks are considered to rotate as a composite block.

[e]This model is where the Wanganui block is allowed to rotate about its own pole, and the rest of the blocks rotate together (as a composite block) about a single pole.

[f]Model A, the WANG and AXIR blocks are independent, while the WAIR, CHKG, and RAUK blocks are a composite block; model B, the WANG, AXIR, and RAUK blocks rotate independently, the WAIR and CHKG blocks are considered a single, composite block.

depth. The strip of apparent high slip rate deficit on the shallow part of the subduction zone offshore the northeastern North Island is a product of this constraint. Whether or not there is a high slip rate deficit in this area is not resolvable with our data set.

6.3. Eastern North Island Block Rotations and Possible Block Strain

[31] We estimate that the eastern North Island is rotating clockwise (as several distinct blocks), with rates varying from 0.5 to 3.8 deg Myr^{-1} relative to the Australian Plate (Figure 7 and Table 3). The poles of rotation for the North Island blocks (with respect to Australia) cluster in a region just west of Taranaki (Figures 3 and 7). This is similar to, but approximately 200 km south of the pole estimated for the eastern North Island from geological strain rate data [*Beanland and Haines*, 1998]. Our poles of rotation are consistent with observations of rifting in the Taupo Volcanic Zone north of 39.5°S [*Villamor and Berryman*, 2001] and shortening south of 39.5°S over the last 5 Myr [*Nicol and Beavan*, 2003; Nicol et al., submitted manuscript, 2004].

[32] We solved for Euler vectors describing the rotation of five adjacent tectonic blocks (Figure 7 and Table 3). The Wairarapa block appears to be rotating most rapidly (3.8 deg Myr^{-1}), while the westernmost blocks are rotating less rapidly (2.9–0.5 deg Myr^{-1}). These rotation rates agree with evidence from geologic strain rates and paleomagnetic data for a decrease in clockwise rotation of tectonic blocks from the eastern to the western North Island [*Wilson and McGuire*, 1995; Nicol et al., submitted manuscript, 2004]. Motion on the eastern North Island upper plate faults facilitates the relative motion between these tectonic slivers.

[33] Much of the North Island appears to behave as relatively coherent, distinct blocks despite the long, narrow shape of the easternmost tectonic slivers. The eastern North Island forearc blocks have residual strain rates ranging from 1 to 35 $\times$ 10^{-9} yr^{-1} (Table 4). For reference, strains of 20 $\times$ 10^{-9} yr^{-1} are equivalent to 1 mm yr^{-1} of differential slip rate over a region the width of the Wairarapa block (50 km). These residual strain rates (Table 4) indicate a low level of internal deformation of the blocks from sources other than slip deficits on the block-bounding faults.

6.4. Predicted Fault Slip Rates in the North Island

6.4.1. Predicted Slip Rates at the Subduction Boundary

[34] The angular velocities that we estimate are used to predict long-term rates of motion across the block boundaries (Figure 10). The highest rates of relative motion are at the Hikurangi Trough. The slip rates range from 60 mm yr^{-1} in the north to 20 mm yr^{-1} (somewhat oblique) at the southern end of the Hikurangi Trough. There is abundant evidence for shortening in the offshore region of the Hikurangi margin, particularly within the accretionary wedge [*Barnes and Mercier de Lepinay*, 1997], and the remainder of the offshore part of the margin [*Lewis and Pettinga*, 1993; *Collot et al.*, 1996]. Therefore much of the convergence occurring at the trench in Figure 10 may actually be distributed among several convergent structures offshore. As there are no GPS velocity estimates for the submarine

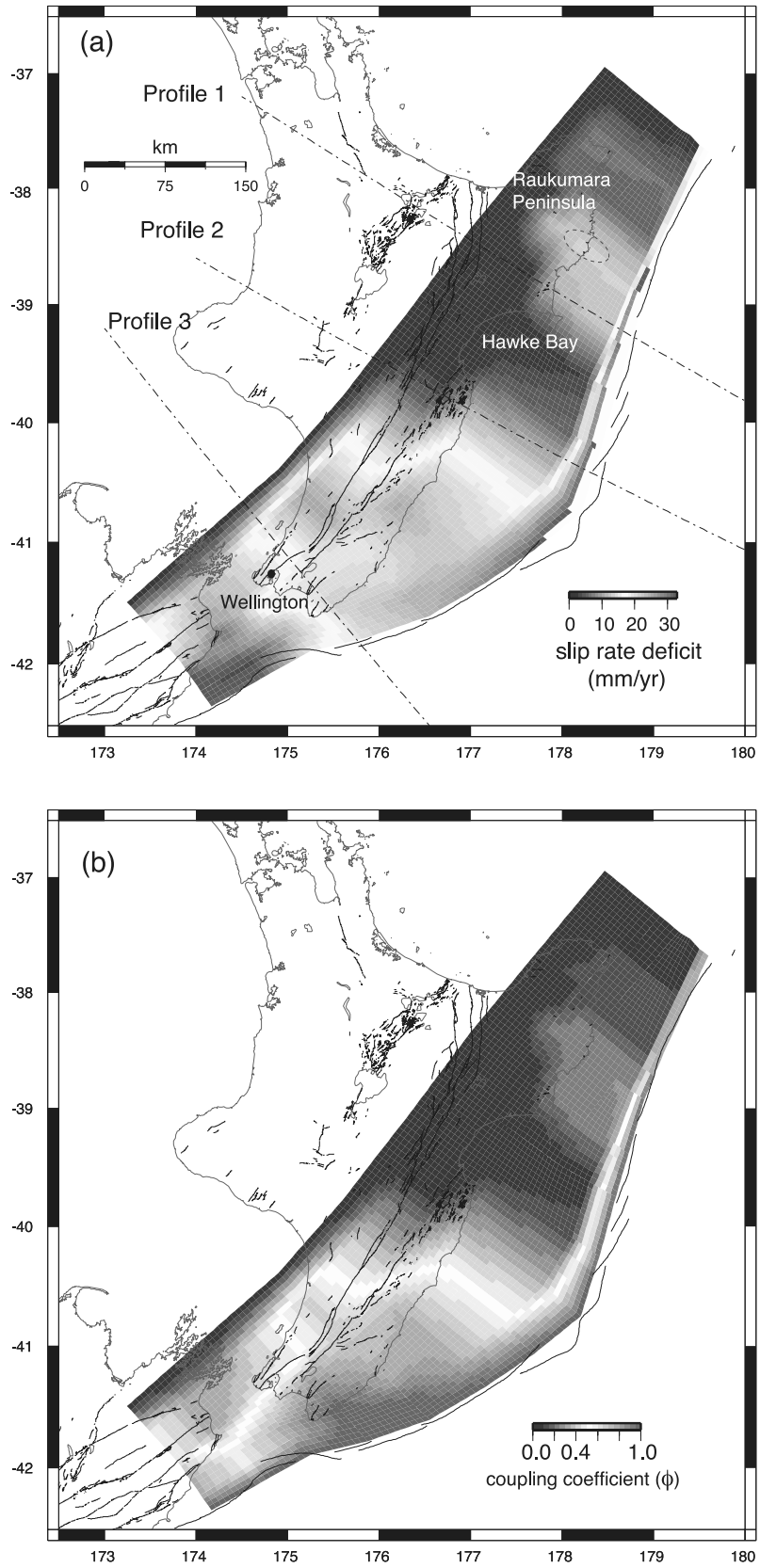

Figure 8. (a) Slip rate deficit (in mm yr^{-1}) on the Hikurangi subduction zone. The dashed ellipse in the Raukumara Peninsula refers to an area of documented high coastal uplift [e.g., *Ota et al.*, 1988, 1992]. Dashed lines refer to the locations of profiles in Figure 11. (b) Value (from 0 to 1) on the subduction interface. The slip rate deficit is multiplied by the relative block motion. See color version of this figure in the HTML.

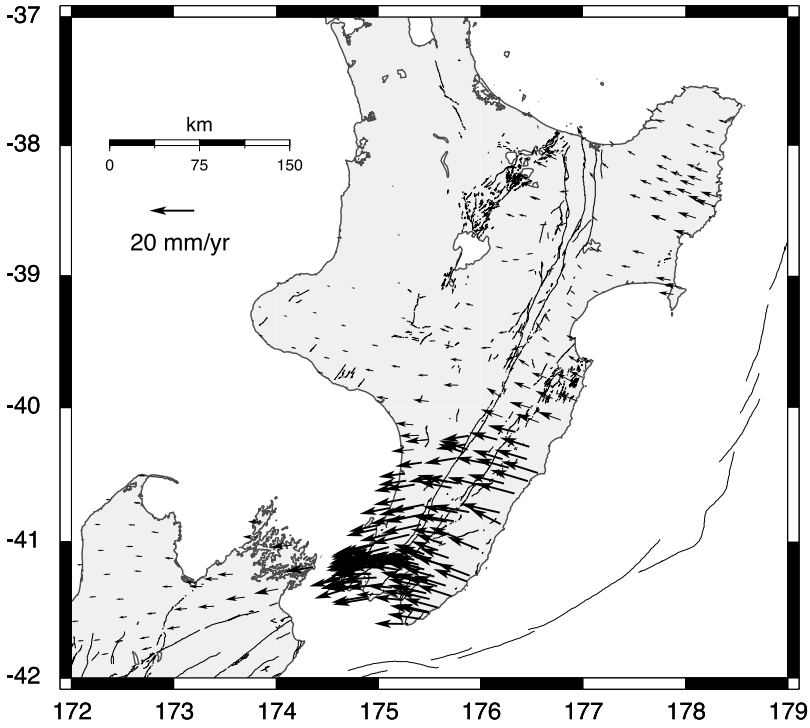

Figure 9. GPS site velocities predicted by elastic strain due to interseismic fault slip deficits (i.e., rotations removed).

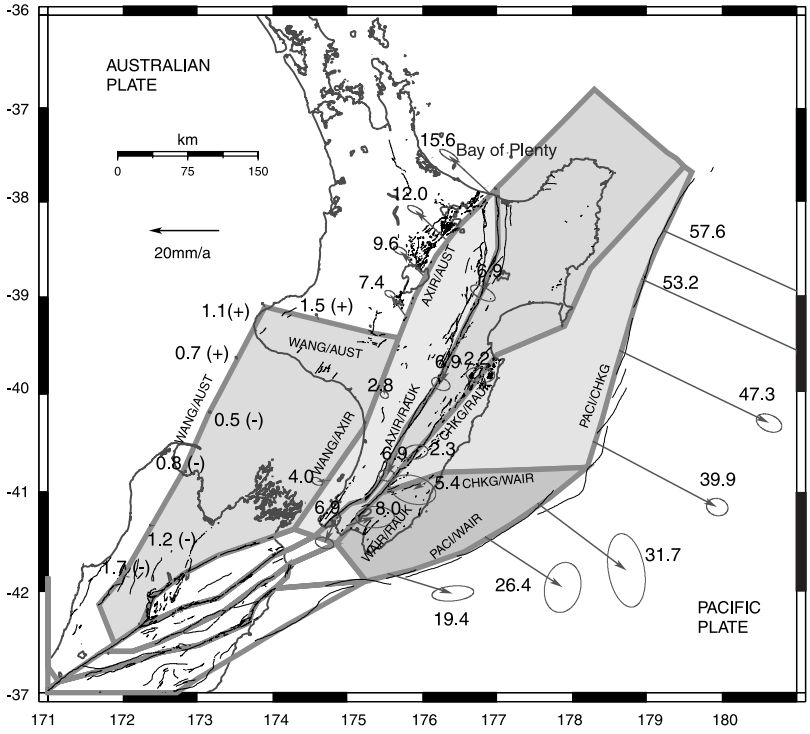

Figure 10. Predicted relative motion (indicated by arrows) across block boundaries (in mm yr^{-1}) based on our kinematic model, with error ellipses showing the uncertainties of the estimates. Plus and minus signify extension and contraction, respectively. At each boundary, we have labeled the two blocks involved in the relative motion. For example, where labeled "WANG/AUST," the motion shown is the Australian Plate movement relative to the Wanganui block (second block named relative to the first block). Key Abbreviations are WANG, Wanganui block; PACI, Pacific Plate; AUST, Australian Plate; WAIR, Wairarapa block; RAUK, Raukumara block; CHKG, Central Hikurangi block; and AXIR, Axial Ranges block. See color version of this figure in the HTML.

portion of the plate boundary, we cannot say how this deformation is distributed through the accretionary wedge structures. There is a dramatic decrease in predicted margin-normal rates of convergence from 41°S (~38 mm yr^{-1}) to 42°S (~10–15 mm yr^{-1}). This decrease in convergence rate is consistent with a distinct narrowing of the accretionary wedge between 41°S and 42°S [*Barnes and Mercier de Lepinay*, 1997].

[35] From the northern end of the margin, and southward to 41°S, the relative motion is perpendicular to the trench, agreeing with inferences of slip partitioning at the Hikurangi margin [*Cashman et al.*, 1992; *Webb and Anderson*, 1998]. However, our kinematic model suggests that relative motion at the Hikurangi Trough becomes more oblique south of 41.5°S. The margin-parallel relative motion that we predict at the Hikurangi Trough south of 41.5°S (from a few to ~15 mm yr^{-1}) may be accommodated on strike-slip structures in the upper plate offshore, rather than as oblique slip on the subduction thrust. For example, a strike-slip fault offshore of the southeastern North Island (Palliser-Kaiwhata fault) could accommodate some of this margin parallel motion, as suggested by *Barnes et al.* [1998]. In any case, an increase in the obliquity of convergence at the southern end of the Hikurangi margin seems likely, as the transition into the strike-slip dominated Marlborough Fault System occurs.

6.4.2. Extension in the Taupo Volcanic Zone

[36] Because of the strong geodetic constraints on the kinematics of the eastern North Island, we can predict the total extension rates in the TVZ, based on the relative motion between the Axial Ranges block and the Australian Plate. We predict a total extension rate of ~15 mm yr^{-1} at the Bay of Plenty, decreasing to <5 mm yr^{-1} at 39°S (Figure 10). In some locations, the extension rates that we predict are twice as high as those documented from paleoseismological studies [e.g., *Villamor and Berryman*, 2001]. Slip on previously unrecognized faults, and processes like dike intrusion must somehow contribute to the remaining extension budget in the TVZ. The kinematics of the eastern North Island constrained by GPS demonstrate that a uniform widening rate for the entire TVZ is not possible, and opening rates must increase from south to north as suggested by other sources of data [e.g., *Stern*, 1987; *Cole et al.*, 1995].

6.4.3. Wellington/Mohaka and Wairarapa Fault Systems

[37] We obtain rates of 7 mm yr^{-1} for the Wellington/Mohaka Fault System, agreeing well with geological estimates varying from 4.0 to 7.6 mm yr^{-1} [*Berryman*, 1990; *Van Dissen et al.*, 1992; *Beanland*, 1995; *Van Dissen and Berryman*, 1996]. This is partly due to the inclusion of long-term geological slip rate data for the Wellington fault in the inversion. However, when we exclude Wellington fault slip rate data, we get similar slip rates (4.3 mm yr^{-1}), indicating that the GPS data are sensitive to the slip on the Wellington fault. This is likely to be true because GPS sites spanning the northern end of the Wellington/Mohaka Fault System are not dominated by elastic strain from subduction zone slip rate deficits (Figures 8 and 9), and therefore are more sensitive to the rate of motion of dextral faults in the northern North Island. Our estimates for slip on the Wairarapa fault (~8 mm yr^{-1} of oblique right-lateral slip) are comparable to the geologically derived estimates of 6–11.5 mm yr^{-1} of right-lateral strike slip [*Van Dissen and Berryman*, 1996; *Grapes*, 1999]. Again, this agreement is expected given that Wairarapa fault slip rate estimates are included in the inversion. When we remove the Wairarapa fault slip rate constraints from the inversion, we obtain a wide range of slip rates for the Wairarapa fault that are inconsistent with the geologically estimated slip rates, but with an equally good fit to the GPS velocities. It is difficult to uniquely estimate rates of activity on the Wairarapa fault with only GPS measurements; this is largely due to the enormous influence of subduction zone coupling on the GPS velocity field in the southern North Island (Figure 9).

6.4.4. Slip on Faults Bounding the Wanganui Block

[38] The northern boundary of the Wanganui block is the Taranaki-Ruapehu line, an ill-understood, likely fault zone, defined by a distinct zone of shallow seismicity [*Reyners*, 1980, 1989] (Figure 4). If the Taranaki-Ruapehu line forms the northern boundary of the Wanganui block, we predict ~1.5 mm yr^{-1} of transtensional (left-lateral) motion. The western boundary of the Wanganui block coincides with a northeast striking extensional fault zone (the Cape Egmont fault zone) identified just offshore of the western North Island and continuing as far south as 40°S [*Nodder*, 1994; *King and Thrasher*, 1996]. This extensional zone projects south-southwest to an area of shortening in the northwestern South Island (Figure 1). On the basis of this change from extension to contraction, *King and Thrasher* [1996] suggested that the Wanganui Basin, northwest Nelson, and southern Taranaki constitute a rigid block rotating (0.2 deg Myr^{-1}) relative to Australia about a pole near 173°E, 40°S. This agrees well with our estimate, although the rotation rates we estimate are slightly higher. On the western boundary of the Wanganui block, the extensional zone to the north, and convergent zone to the south are defined by a line of shallow seismicity (Figure 4) [*Anderson and Webb*, 1994]. There is a gap in seismicity near where the rates of relative motion across the western boundary of the Wanganui block decrease to zero (Figures 4 and 10). We predict ~1 mm yr^{-1} of extension on the western boundary of the Wanganui block at 39°S, decreasing to zero near 40°S, and changing to contraction in the Buller region of the northwestern South Island at rates of 0.5–2 mm yr^{-1} between 40°S and 42°S in the northwestern South Island (Figure 10). The shortening we predict in the northwestern South Island from our block model is consistent with thrust earthquakes observed in the Buller region in the last century at Inangahua (1968, M_w = 7.1) and Murchison (1929, M_s = 7.8) [*Dowrick and Smith*, 1990; *Anderson et al.*, 1993, 1994].

[39] The oblique shortening predicted at the eastern boundary of the Wanganui block can be correlated with a distributed zone of shortening in the eastern Wanganui Basin, an area known as the Kapiti-Manawatu Fault System [*Melhuish et al.*, 1996; *Jackson et al.*, 1998; *LaMarche et al.*, 2003], and active strike slip on faults such as the Ohariu Fault [e.g., *Heron et al.*, 1998]. We predict ~1–4 mm yr^{-1} of oblique shortening in this area.

6.4.5. Central Hikurangi Block and Implications for Activity on the Carterton and Masterton Faults

[40] At early stages in our analysis, we treated the Central Hikurangi and Wairarapa blocks as a single, composite block. However, this produced results that disagree with the geological estimates of fault slip rates and directions

on the western boundary of the composite block. The Wairarapa fault from the latitude of Wellington to 41°S is well determined from paleoseismological and stream terrace offset studies to have a right-lateral strike-slip rate of 8–11 mm yr^{-1} [see *Van Dissen and Berryman*, 1996; *Grapes*, 1999, and references therein], and it probably has some component of shortening as well. However, the strike-slip rates on the northeastward continuation of the Wairarapa fault decrease north of 41°S to 2.6 ± 1.5 mm yr^{-1} [*Beanland and Haines*, 1998], and slow shortening dominates structures in the southern Hawke's Bay region [*Kelsey et al.*, 1998].

[41] To satisfy the geological slip rate estimates, it is implausible for the Wairarapa and Central Hikurangi blocks to be the same tectonic block. If the entire fault system extending from the Wairarapa fault northeastward toward Hastings changes from a strike-slip dominated regime to a convergent system, the Euler vector describing the motion between a composite Central Hikurangi/Wairarapa block and the sliver to the west (the Raukumara block) must be southeast of the Wairarapa block. If the Euler vector describing the motion of the Central Hikurangi/Wairarapa block relative to the Raukumara block is southeast of the Wairarapa block, rates on the Wairarapa and related faults must increase northward toward Hastings (Figure 3), contrary to the geologic evidence. Likewise, to match the slow shortening rates (0.4–1.4 mm yr^{-1}) observed near Hastings [*Kelsey et al.*, 1998], and higher rates of faulting on the Wairarapa fault at the latitude of Wellington (8–11 mm yr^{-1}), the Euler vector between a composite Central Hikurangi/Wairarapa block and the Raukumara block must lie close to Hastings, resulting in shortening (with no strike slip) on the Wairarapa fault further south; this is also incompatible with the geologic evidence.

[42] In order to satisfy the geological evidence, we found it necessary to split the Central Hikurangi/Wairarapa composite block into two distinct blocks. The most likely boundary between these two blocks is along the Carterton, Masterton, and Mokonui faults, part of a northeasterly trending fault system projecting toward the coast from the Wairarapa fault near Masterton (Figure 3). These faults are morphologically well defined and appear to be active, and dominated by right-lateral strike slip, with some possible normal faulting components [*Zachariasen et al.*, 2000; *Begg et al.*, 2001; *Townsend et al.*, 2002; *Langridge et al.*, 2003]. The slip rates of these faults are largely unknown, but *Zachariasen et al.* [2000] suggest a minimum of 2–4 mm yr^{-1} (right-lateral strike slip) is possible for the Carterton fault. Our kinematic model predicts approximately 5 mm yr^{-1} of right-lateral strike slip and slow (<1 mm yr^{-1}) extension (Figure 10) on this fault system. We suggest that slip on these faults allow some of the high strike-slip rates to be transferred away from the Wairarapa fault, thus producing a northward decrease in slip within the North Island Dextral fault belt.

6.5. Slip Partitioning at the Hikurangi Margin

[43] Our results agree with the suggestion that slip partitioning occurs in the North Island [e.g., *Cashman et al.*, 1992; *Webb and Anderson*, 1998; *Barnes et al.*, 1998]. However, the manner in which slip partitioning occurs in the North Island of New Zealand is quite different from the more commonly cited case of slip partitioning in Sumatra. In the Sumatra-style concept of slip partitioning, the margin-normal component of relative motion occurs on the subduction interface, and most (or all) of the margin-parallel component is taken up on strike-slip faults within the upper plate [e.g., *Fitch*, 1972; *McCaffrey*, 1992]. The opposite end of the spectrum (i.e., no slip partitioning) would be the occurrence of oblique slip on the subduction interface, with no faulting in the upper plate. In Sumatra, approximately 2/3 of the margin-parallel component of motion is accommodated by upper plate strike slip faults, while 1/3 of the margin-parallel motion is taken up by oblique slip on the subduction interface [*McCaffrey et al.*, 2000b]. In cases where most of the margin-parallel component of motion is accommodated by strike-slip faulting along the arc, the convergent plate boundary microblock (CPBM) rotates relative to the upper and lower plates about a distant pole of rotation.

[44] Previous workers [e.g., *Cashman et al.*, 1992; *Kelsey et al.*, 1995] have treated New Zealand as a "Sumatra-type" margin, but the rates of strike slip required to accommodate Pacific-Australia relative motion are much greater than those documented on upper plate strike slip faults. For example, strike slip on known faults may amount to 6 mm yr^{-1} in the northern North Island and 21 mm yr^{-1} in the southern North Island [*Beanland*, 1995; *Van Dissen and Berryman*, 1996]. The total margin-parallel component of slip between the Pacific and Australian plates is 31 mm yr^{-1} near 41°S and 25 mm yr^{-1} near 38°S (Figures 1 and 11). This is 10–19 mm yr^{-1} higher than rates estimated on known strike-slip faults in the North Island. Earthquake slip vectors on the subduction interface indicate slip partitioning occurs for most of the Hikurangi margin [*Webb and Anderson*, 1998]. Unless there are undiscovered strike-slip faults with high slip rates on the Hikurangi margin, another mechanism must be called on to accommodate this margin-parallel component of motion.

[45] The GPS velocity field shows rotation of much of the North Island (Figure 2). The clockwise rotation of the eastern North Island is an alternative means of accommodating across-margin gradients in margin-parallel relative plate motion [*Beanland and Haines*, 1998]. From our estimates of North Island block kinematics, it is possible to accommodate 25–65% of the margin-parallel Australia-Pacific relative motion in the North Island by rotation (Figure 11). Our estimation of the margin-parallel component of relative motion due to block rotations at various points along the margin is illustrated in Figure 11b, where the relative contributions of block rotations can be discerned from the sloping portion of the profile (margin-parallel component, grey profile line) between the block boundaries, and the contribution from faulting is denoted by the steps in the profile at the block boundaries. The net effect of this rotation is extension in the TVZ, and distributed shortening south of the TVZ (e.g., Kapiti-Manawatu Fault System, and the Buller region of the northwestern South Island), without requiring large amounts of strike slip in the upper plate. Nicol et al. (submitted manuscript, 2004) use geologic shortening and extension rates, and paleomagnetic evidence to estimate rotations, to come to a similar conclusion concerning the

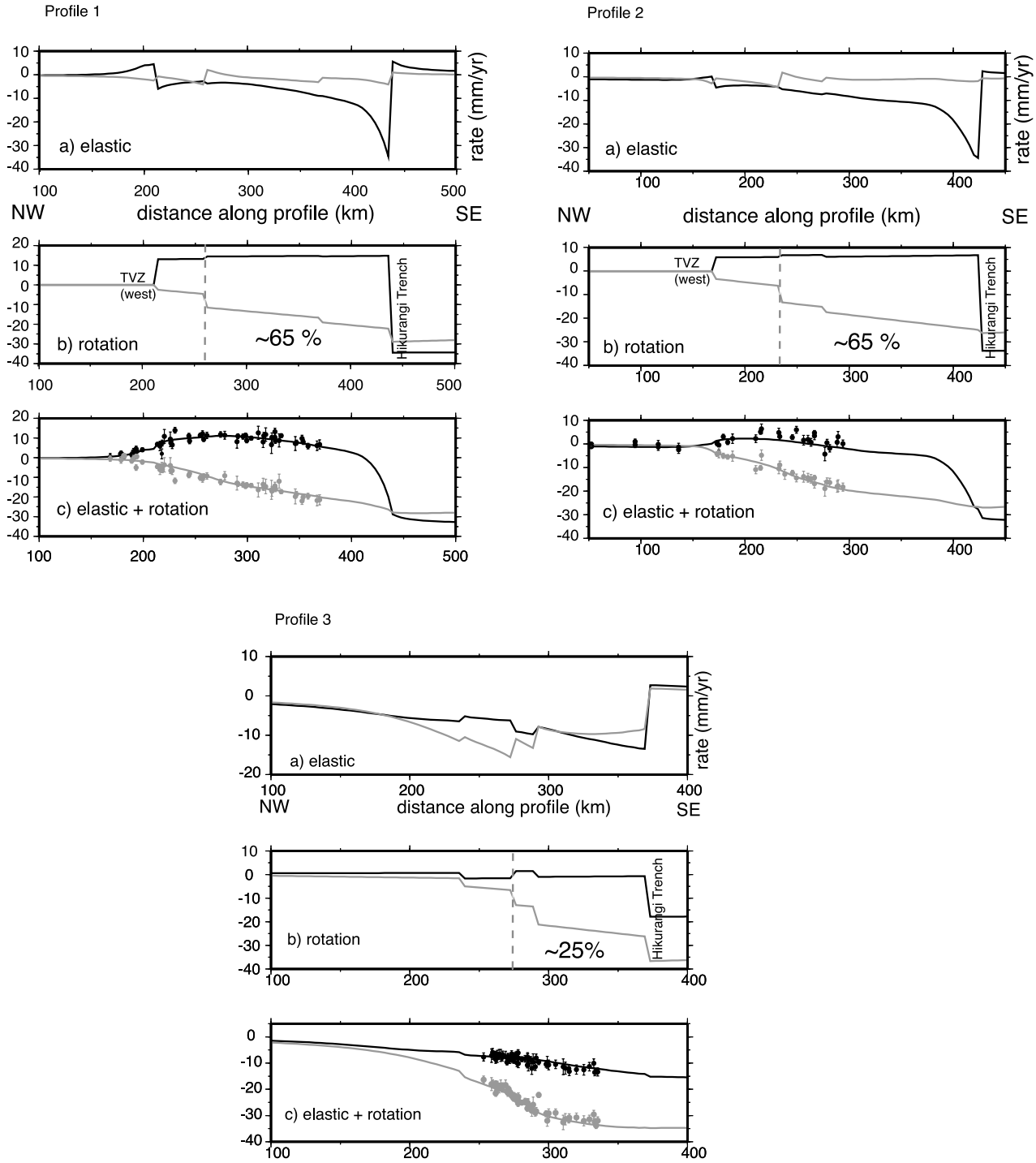

Figure 11. Profiles normal to the Hikurangi Margin showing the margin-parallel (grey) and margin-perpendicular (black) components of the (a) elastic, (b) rotational, and (c) combined elastic and rotational velocity components plus the GPS velocity data projected onto the profiles. Locations of the profile lines are shown in Figure 9. Key features to note in the rotational component are steps in the profile where there are faults and the slope of the lines between the faults indicating contribution from block rotations to relative plate motion. Percentage of margin-parallel relative motion accommodated by rotation is denoted in the box containing the rotation profiles. In all cases, 0 mm yr^{-1} on the y axis corresponds to Australian Plate motion, so largest negative values will be closest to Pacific Plate motion. The light gray, vertical dashed line shows where the profiles cross the Wellington/Mohaka Fault System. TVZ (west) corresponds to the western boundary of the TVZ.

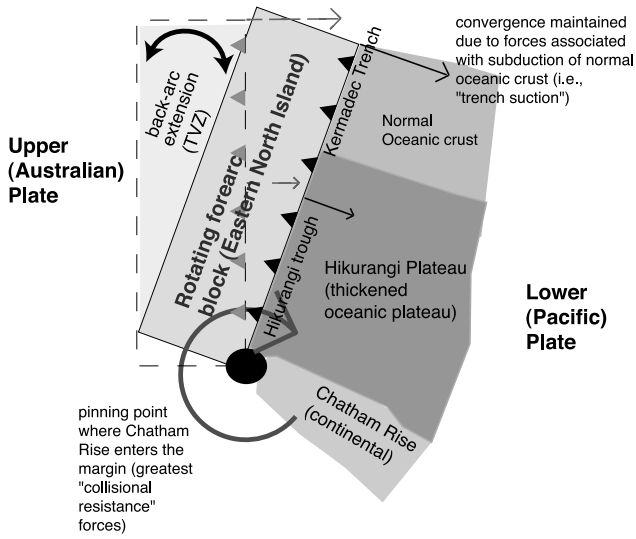

Figure 12. Schematic of our proposed mechanism for the rotation of the eastern North Island. See color version of this figure in the HTML.

role of the eastern North Island rotation in the slip partitioning process. Another location where tectonic rotation assists in this process is at the Cascadia margin, where the rotation of Oregon accommodates most of the margin-parallel component of motion between the Juan De Fuca and North American plates [*Wells et al.*, 1998; *McCaffrey et al.*, 2000a]. It may be that CPBM rotation is a common means of enabling slip partitioning: Sumatra-style slip partitioning may actually be the exception, rather than the rule.

6.6. A Mechanism for Rotation of the Eastern North Island

[46] The poles of rotation of the North Island tectonic blocks (with the exception of the Wanganui block) relative to the Pacific plate cluster in the region where the Chatham Rise impinges upon the margin (Figure 1 and Table 3). The Chatham Rise is a continental fragment, and is essentially "unsubductable." Northward, the Chatham Rise becomes the Hikurangi Plateau, a thickened oceanic plateau that is ~15 km thick beneath the southern North Island [*Robinson*, 1986; *Davy and Wood*, 1994]. *Bannister* [1988] estimates the plateau thickness to be 10–12 km in the Hawkes Bay region, and *Davy and Wood* [1994] estimate a 10 km thickness for the northern portion of the plateau, east of the Raukumara Peninsula. This plateau eventually changes to normal oceanic crust (5–7 km thick), subducting at the Kermadec Trench north of 36°S [*Davy*, 1992]. We suggest that it is these along-strike variations in the thickness (and buoyancy) of the subducting plate that dictate the kinematics of the tectonic block rotations in the North Island.

[47] The cause of back-arc opening is widely debated, and many origins for this phenomenon have been proposed [e.g., *Elsasser*, 1971; *Karig*, 1971; *Chase*, 1978; *Molnar and Atwater*, 1978; *Uyeda and Kanamori*, 1979; *Taylor and Karner*, 1983]. Although still unresolved, the most widely cited cause for back-arc rifting is rollback of a negatively buoyant subducting slab [e.g., *Molnar and Atwater*, 1978; *Dewey*, 1980; *Royden*, 1993; *Lonergan and White*, 1997; *Wortel and Spakman*, 2000; *Schellart et al.*, 2002]. If rollback occurs, upper plate microblocks (often coinciding with the forearc) will keep up with the seaward migration of the trench hingeline because of "trench suction" [e.g., *Elsasser*, 1971; *Shemenda*, 1993], causing extension to occur in the back-arc region. The oceanic crust subducting at the Kermadec trench is relatively old, probably early to mid-Cretaceous [*Bradshaw*, 1989], and rollback of the negatively buoyant oceanic slab here is possible [e.g., *Molnar and Atwater*, 1978]. At the southern end of the North Island, where the Hikurangi plateau becomes thicker and more buoyant, "colliding resistance" forces [e.g., *Forsyth and Uyeda*, 1975] inhibit the convergence between the upper plate and the subducting Pacific plate. The competing forces ("collisional resistance" and "trench suction"), which are spatially distributed along the plate boundary, effectively exert a torque on the eastern North Island causing it to rotate about a nearby axis (Figure 12). A similar mechanism for microplate rotation has been proposed in Papua New Guinea, where the southern boundary of the South Bismarck microplate changes from arc-continent collision to subduction at the New Britain Trench [*Wallace et al.*, 2004].

[48] The "colliding resistance" forces will be highest where the thick and buoyant Chatham Rise intersects the margin. The eastern North Island blocks rotate relative to the Pacific Plate about poles of rotation adjacent to where the Chatham Rise impinges on the margin (Figures 1 and 12 and Table 3). Consequently, the kinematics of the eastern North Island relative to the subducting Pacific plate is largely determined by where the thick, unsubductable Chatham Rise enters the margin (Figure 1). The detailed kinematics of TVZ opening reflects the relative motion between the mobile North Island tectonic blocks and the Australian Plate. This is determined by two things: (1) the relative motion between the eastern North Island and the Pacific plate, dictated by the changing subduction zone boundary condition as discussed above and (2) the relative motion between the Pacific and Australian plates, determined by larger-scale plate tectonic processes.

7. Conclusions

[49] We fit GPS, earthquake, and geologic data within uncertainties in the North Island of New Zealand using elastic, rotating blocks. In agreement with previous studies [*McCaffrey et al.*, 2000a; *McClusky et al.*, 2001; *McCaffrey*, 2002; *Wallace et al.*, 2004], this result suggests that a tectonic block approach to the interpretation of geodetic data is plausible for plate boundary zones. Our results also emphasize the importance of accounting for geological and seismological information when interpreting GPS velocity fields.

[50] The deformation in the North Island is dominated by several tectonic blocks that rotate at approximately 0.5–3.8 deg Myr^{-1} relative to the Australian Plate, and elastic strain from spatially variable interseismic slip rate deficits on the Hikurangi subduction zone interface. The ϕ distribution on the subduction zone decreases from nearly 1.0 in the southern North Island to smaller values (a lower slip rate deficit) in the northeastern North Island. This ϕ distribution agrees with inferences from previous seismo-

logical and geodetic studies [*Walcott*, 1984; *Reyners*, 1998; *Darby and Beavan*, 2001], but our inversion provides higher spatial resolution. We also note a small patch with a significant slip rate deficit beneath the Raukumara Peninsula. This study provides the first detailed estimate of the interseismic slip rate deficit on the Hikurangi subduction zone, and therefore has implications for understanding seismic hazards posed by the subduction zone in the North Island.

[51] Tectonic blocks in the eastern North Island appear to behave coherently, allowing us to predict fault slip rates in the region based on the relative tectonic block motions. Block rotations in the North Island accommodate ~25–65% of the margin parallel component of Pacific/Australia relative motion. In contrast to the South Island of New Zealand, where strike-slip faulting dominates, we see no evidence for high rates of strike-slip faulting in the North Island despite the fact that the margin-parallel component of Pacific-Australia relative motion reaches 31 mm yr^{-1} in the southern North Island. It is also likely that some of this margin-parallel motion at the far southern end of the Hikurangi Margin is taken up as oblique slip on the subduction interface. However, the relative motion on the subduction interface is perpendicular to the trench north of 41.5 S, agreeing with inferences of slip partitioning at the Hikurangi margin. This result highlights the importance of tectonic block rotation about a nearby axis in the process of slip partitioning, and should be considered when assessing these processes at other obliquely convergent margins.

[52] We suggest that tectonic block rotation in the North Island occurs due to the change in character of the subducting plate along the margin. The subducting Hikurangi Plateau is thicker and more buoyant in the south compared to the north. Collisional resistance forces will be high in the southern Hikurangi margin, while rollback of the slab (and trench suction) may occur at the northern end where oceanic crust is subducted. This variation in boundary condition along the Hikurangi margin applies a torque to the eastern North Island, causing it to rotate clockwise about a nearby axis. This mechanism for convergent margin tectonic block rotation is similar to that suggested for block rotations in Papua New Guinea [*Wallace et al.*, 2004]. This could be an important, globally widespread mechanism for producing rapid block rotations at convergent margins.

[53] **Acknowledgments.** The funding for this work was provided by the Foundation for Research Science and Technology (FRST), New Zealand. GPS data were collected by numerous individuals, principally from the Institute of Geological and Nuclear Sciences (GNS) and also from DOSLI, LDEO, UNAVCO, and occasional volunteers. McCaffrey's participation was supported by GNS, a sabbatical from Rensselaer Polytechnic Institute, and NSF grant EAR-0230054. This work benefited greatly from discussions with John Begg, Kelvin Berryman, Ursula Cochran, Hugh Cowan, Susan Ellis, Andy Nicol, Martin Reyners, Steve Sherburn, Mark Stirling, Russ Van Dissen, and Pilar Villamor. Reviews of an earlier version of this manuscript by Kelvin Berryman and Andy Nicol improved it substantially. The paper also benefited from careful reviews by Tim Dixon, Juergen Klotz, Jim Savage, and Associate Editor Kelin Wang. Many of the figures in this paper were made using Generic Mapping Tools software [*Wessel and Smith*, 1995]. GNS contribution 3144.

References

Anderson, H., and T. Webb (1994), New Zealand seismicity: Patterns revealed by the upgraded National Seismograph Network, *N. Z. J. Geol. Geophys.*, *37*, 477–493.

Anderson, H., T. Webb, and J. Jackson (1993), Focal mechanisms of large earthquakes in the South Island of New Zealand: Implications for the accommodation of Pacific-Australia plate motion, *Geophys. J. Int.*, *115*, 1032–1054.

Anderson, H., S. Beanland, G. Blick, D. Darby, G. Downes, J. Haines, J. Jackson, R. Robinson, and T. Webb (1994), The 1968 May 23 Inangahua, New Zealand, earthquake: An integrated geological, geodetic and seismological source model, *N. Z. J. Geol. Geophys.*, *37*, 59–86.

Ansell, J. H., and S. C. Bannister (1996), Shallow morphology of the subducted Pacific plate along the Hikurangi margin, New Zealand, *Phys. Earth Planet. Inter.*, *93*, 3–20.

Bannister, S. (1988), Microseismicity and velocity structure in the Hawkes Bay region, New Zealand: Fine structure of the subducting Pacific plate, *Geophys. J. R. Astron. Soc.*, *95*, 45–62.

Barnes, P. M., and B. Mercier de Lepinay (1997), Rates and mechanics of rapid frontal accretion along the very obliquely convergent southern Hikurangi margin, New Zealand, *J. Geophys. Res.*, *102*, 24,931–24,952.

Barnes, P. M., B. Mercier de Lepinay, J. Y. Collot, J. Delteil, and J. C. Audru (1998), Strain partitioning in the transition area between oblique subduction and continental collision, Hikurangi margin, New Zealand, *Tectonics*, *17*, 534–557.

Beanland, S. (1995), The North Island dextral fault belt, Hikurangi subduction margin, New Zealand, Ph.D. thesis, Victoria Univ. of Wellington, Wellington.

Beanland, S., and J. Haines (1998), The kinematics of active deformation in the North Island, New Zealand, determined from geological strain rates, *N. Z. J. Geol. Geophys.*, *41*, 311–323.

Beavan, J., and J. Haines (2001), Contemporary horizontal velocity and strain-rate fields of the Pacific-Australian plate boundary zone through New Zealand, *J. Geophys. Res.*, *106*, 741–770.

Beavan, J., M. Moore, C. Pearson, M. Henderson, B. Parsons, S. Bourne, P. England, D. Walcott, G. Blick, D. Darby, and K. Hodgkinson (1999), Crustal deformation during 1994–1998 due to oblique continental collision in the central Southern Alps, New Zealand, and implications for seismic potential of the Alpine fault, *J. Geophys. Res.*, *104*, 25,233–25,255.

Beavan, J., P. Tregoning, M. Bevis, T. Kato, and C. Meertens (2002), Motion and rigidity of the Pacific Plate and implications for plate boundary deformation, *J. Geophys. Res.*, *107*(B10), 2261, doi:10.1029/2001JB000282.

Begg, J., P. Villamor, J. Zachariasen, and N. Litchfield (2001), Paleoseismic assessment of the active Masterton and Carterton faults, Wairarapa, *Client Rep.2001/70*, 32 pp., Inst. of Geol. and Nucl. Sci., Lower Hutt, N. Z.

Berryman, K. (1990), Quaternary movement on the Wellington Fault in the Lower Hutt area, New Zealand, *N. Z. J. Geol. Geophys.*, *33*, 257–270.

Beutler, G., et al. (2001), Bernese GPS software version 4.2, Astron. Inst., Univ. of Bern, Bern, Switzerland.

Bibby, H. M. (1973), The reduction of geodetic survey data for the detection of Earth deformation, *DSIR Geophys. Div. Rep.84*, 31 pp., Dep. of Sci. and Ind. Res., Wellington.

Bibby, H. M. (1981), Geodetically determined strain across the southern end of the Tonga-Kermadec-Hikurangi subduction zone, *Geophys. J. R. Astron. Soc.*, *66*, 513–533.

Bibby, H. M. (1982), Unbiased estimate of strain from triangulation data using the method of simultaneous reduction, *Tectonophysics*, *82*(1–2), 161–174.

Bradshaw, J. D. (1989), Cretaceous geotectonic patterns in the New Zealand region, *Tectonics*, *8*, 803–820.

Calmant, S., B. Pelletier, P. Lebellegard, M. Bevis, F. W. Taylor, and D. Phillips (2003), New insights on the tectonics along the New Hebrides subduction zone based on GPS results, *J. Geophys. Res.*, *108*(B6), 2319, doi:10.1029/2001JB000644.

Cashman, S. M., H. M. Kelsey, C. F. Erdman, H. N. C. Cutten, and K. R. Berryman (1992), Strain partitioning between structural domains in the forearc of the Hikurangi subduction zone, New Zealand, *Tectonics*, *11*, 242–257.

Chase, C. G. (1978), Extension behind island arcs and motions relative to hot spots, *J. Geophys. Res.*, *83*, 5385–5387.

Cole, J. W., D. J. Darby, and T. A. Stern (1995), Taupo Volcanic Zone and Central Volcanic Region backarc structures of North Island, New Zealand, in *Backarc Basins: Tectonics and Magmatism*, edited by B. Taylor, pp. 1–24, Plenum, New York.

Collot, J. Y., et al. (1996), From oblique subduction to intracontinental transpression: Structures of the southern Kermadec Hikurangi margin from multibeam bathymetry, side scan sonar and seismic reflection, *Mar. Geophys. Res.*, *18*, 357–381.

Collot, J. Y., K. Lewis, G. Lamarche, and S. Lallemand (2001), The giant Ruatoria debris avalanche on the northern Hikurangi margin,

New Zealand: Result of oblique seamount subduction, *J. Geophys. Res.*, *106*, 19,271–19,297.
Crook, C. N. (1992), ADJCOORD: A FORTRAN program for survey adjustment and deformation modelling, *NZGS EDS Rep.138*, Dep. of Sci. and Ind. Res. Geol. and Geophys., Lower Hutt, N. Z.
Darby, D. J., and J. Beavan (2001), Evidence from GPS measurements for contemporary plate coupling on the southern Hikurangi subduction thrust and partitioning of strain in the upper plate, *J. Geophys. Res.*, *106*, 30,881–30,891.
Davy, B. W. (1992), The influence of subducting plate buoyancy on subduction of the Hikurangi-Chatham Plateau beneath the North Island, New Zealand, in *Advances in the Geology and Geophysics of the Continental Margin*, edited by J. Watkins, F. Zhigiang, and K. McMillen, *AAPG Mem.*, *53*, 75–91.
Davy, B., and R. Wood (1994), Gravity and magnetic modeling of the Hikurangi Plateau, *Mar. Geol.*, *118*, 139–151.
DeMets, C., R. G. Gordon, D. F. Argus, and S. Stein (1990), Current plate motions, *Geophys. J. Int.*, *101*, 425–478.
DeMets, C., R. G. Gordon, D. F. Argus, and S. Stein (1994), Effects of recent revisions to the geomagnetic reversal time scale on estimates of current plate motions, *Geophys. Res. Lett.*, *21*, 2191–2194.
Dewey, J. F. (1980), Episodicity, sequence and style at convergent plate boundaries, in *The continental Crust and Its Mineral Resources*, edited by D. Strangway, *Spec. Pap. Geol. Assoc. Can.*, *20*, 1980, 553–574.
Doser, D. I., and T. Webb (2003), Source parameters of large historical (1917–1961) earthquakes, North Island, New Zealand, *Geophys. J. Int.*, *152*, 795–832.
Doser, D. I., T. H. Webb, and D. E. Maunder (1999), Source parameters of large historic (1918–1962) earthquakes, South Island, New Zealand, *Geophys. J. Int.*, *139*, 769–794.
Dowrick, D. J., and E. G. C. Smith (1990), Surface wave magnitudes of some New Zealand earthquakes, 1901–1988, *Bull. N. Z. Natl. Soc. Earthquake Eng.*, *23*, 198–219.
Elsasser, W. M. (1971), Sea-floor spreading as thermal convection, *J. Geophys. Res.*, *76*, 1101–1112.
Fitch, T. J. (1972), Plate convergence, transcurrent faults, and internal deformation adjacent to Southeast Asia and the western Pacific, *J. Geophys. Res.*, *77*, 4432–4460.
Forsyth, D., and S. Uyeda (1975), On the relative importance of the driving forces of plate motion, *Geophys. J. R. Astron. Soc.*, *43*, 163–200.
Grapes, R. H. (1999), Geomorphology of faulting: The Wairarapa Fault, New Zealand, *Z. Geomorph.*, *115*, 191–217.
Heron, D. W., R. J. Van Dissen, and M. Sawa (1998), Late Quaternary movement on the Ohariu Fault, Tongue Point to MacKays Crossing, North Island, New Zealand, *N. Z. J. Geol. Geophys.*, *41*, 419–439.
Holt, W. E., and A. J. Haines (1995), The kinematics of northern South Island, New Zealand, determined from geologic strain rates, *J. Geophys. Res.*, *100*, 17,991–18,010.
Jackson, J., R. Van Dissen, and K. Berryman (1998), Tilting of active folds and faults in the Manawatu region, New Zealand: Evidence from surface drainage patters, *N. Z. J. Geol. Geophys.*, *41*, 377–385.
Karig, D. E. (1971), Origin and development of marginal basins in the western Pacific, *J. Geophys. Res.*, *76*, 2542–2561.
Kato, T., J. Beavan, T. Matsushima, Y. Kotake, J. T. Camacho, and S. Nakao (2003), Geodetic evidence of back-arc spreading in the Mariana Trough, *Geophys. Res. Lett.*, *30*(12), 1625, doi:10.1029/2002GL016757.
Kelsey, H. M., S. M. Cashman, S. Beanland, and K. R. Berryman (1995), Structural evolution along the inner forearc of the obliquely convergent Hikurangi margin, New Zealand, *Tectonics*, *14*, 1–18.
Kelsey, H. M., A. G. Hull, S. M. Cashman, K. R. Berryman, P. H. Cashman, J. H. Trexler, and J. G. Begg (1998), Paleoseismology of an active reverse fault in a forearc setting: The Poukawa fault zone, Hikurangi forearc, New Zealand, *Geol. Soc. Am. Bull.*, *110*(9), 1123–1148.
King, P., and G. P. Thrasher (1996), Cretaceous-Cenozoic geology and petroleum systems of the Taranaki Basin, New Zealand, *Inst. Geol. Nucl. Sci. Monogr.*, *13*.
LaMarche, G., S. D. Nodder, and J. Proust (2003), Constraining fault interactions and vertical displacement rates in a compressive proto-back-arc environment, South Wanganui Basin, New Zealand, *Eos Trans. AGU*, *84*(46), Fall Meet. Suppl., Abstract T21E-05.
Langridge, R. M., D. Townsend, and M. Persaud (2003), Paleoseismic assessment of the active Mokonui Fault, Wairarapa, *Client Rep.2003/68*, 35 pp., Inst. of Geol. and Nucl. Sci., Lower Hutt, N. Z.
Lay, T., and S. Y. Schwartz (2004), Comment on "Coupling semantics and science in earthquake research," *Eos Trans. AGU*, *85*(36), 339–340.
Lewis, K. B., and J. R. Pettinga (1993), The emerging, imbricated frontal wedge of the Hikurangi margin, in *South Pacific Sedimentary Basins*, vol. 2, *Sedimentary Basins of the World*, edited by P. F. Balance, pp. 225–250, Elsevier Sci., New York.
Lonergan, L., and N. White (1997), Origin of the Betic-Rif mountain belt, *Tectonics*, *16*, 504–522.
McCaffrey, R. (1992), Oblique plate convergence, slip vectors, and forearc deformation, *J. Geophys. Res.*, *97*, 8905–8915.
McCaffrey, R. (1995), DEF-NODE users guide, Rensselaer Polytech. Inst., Troy, N. Y.
McCaffrey, R. (2002), Crustal block rotations and plate coupling, in *Plate Boundary Zones*, *Geodyn. Ser.*, vol. 30, edited by S. Stein and J. Freymueller, pp. 100–122, AGU, Washington, D. C.
McCaffrey, R., M. D. Long, C. Goldfinger, P. C. Zwick, J. L. Nabelek, C. K. Johnson, and C. Smith (2000a), Rotation and plate locking at the southern Cascadia subduction zone, *Geophys. Res. Lett.*, *27*, 3117–3120.
McCaffrey, R., P. C. Zwick, Y. Bock, L. Prawirodirdjo, J. F. Genrich, C. W. Stevens, S. S. O. Puntodewo, and C. Subaraya (2000b), Strain partitioning during oblique plate convergence in northern Sumatra: Geodetic and seismologic constraints and numerical modeling, *J. Geophys. Res.*, *105*, 28,363–28,376.
McClusky, S., et al. (2001), Present-day kinematics of the eastern California shear zone from a geodetically constrained block model, *Geophys. Res. Lett.*, *28*, 3369–3372.
Meade, B. J., and B. H. Hager (1999), Simultaneous inversions of geodetic and geologic data for block motions in plate boundary zones, *Eos Trans. AGU*, *80*(46), Fall Meet. Suppl., F267–F268.
Melhuish, A., R. Van Dissen, and K. Berryman (1996), Mount Stewart-Halcombe Anticline: A look inside a growing fold in the Manawatu region, New Zealand, *N. Z. J. Geol. Geophys.*, *39*, 123–133.
Molnar, P., and T. Atwater (1978), Interarc spreading and Cordilleran tectonics as alternatives related to the age of the subducted oceanic lithosphere, *Earth Planet. Sci. Lett.*, *41*, 330–340.
Nicol, A., and J. Beavan (2003), Shortening of an overriding plate and its implications for slip on a subduction thrust, central Hikurangi Margin, New Zealand, *Tectonics*, *22*(6), 1070, doi:10.1029/2003TC001521.
Nicol, A., R. Van Dissen, P. Vella, B. Alloway, and A. Melhuish (2002), Growth of contractional structures during the last 10 m.y. at the southern end of the emergent Hikurangi forearc basin, New Zealand, *N. Z. J. Geol. Geophys.*, 365–385.
Nodder, S. D. (1994), Characterizing potential offshore seismic sources using high-resolution geophysical and seafloor sampling programs: An example from Cape Egmont fault zone, Taranaki shelf, New Zealand, *Tectonics*, *13*, 641–658.
Norris, R. J., and A. F. Cooper (2000), Late Quaternary slip rates and slip partitioning on the Alpine Fault, New Zealand, *J. Struct. Geol.*, *23*, 507–520.
Okada, Y. (1985), Surface deformation to shear and tensile faults in a half-space, *Bull. Seismol. Soc. Am.*, *75*, 1135–1154.
Ota, Y., K. R. Berryman, A. G. Hull, T. Miyauchi, and N. Iso (1988), Age and height distribution of Holocene transgressive deposits in eastern North Island, New Zealand, *Palaeogeogr. Palaeoclimatol. Palaeoecol.*, *68*, 135–151.
Ota, Y., A. G. Hull, N. Iso, Y. Ikeda, I. Moriya, and T. Yoshikawa (1992), Holocene marine terraces on the northeast coast of North Island, New Zealand, and their tectonic significance, *N. Z. J. Geol. Geophys.*, *35*, 273–288.
Prawirodirdjo, L., et al. (1997), Geodetic observations of interseismic strain segmentation at the Sumatra subduction zone, *Geophys. Res. Lett.*, *24*, 2601–2604.
Press, W. H., B. P. Flannery, S. A. Teukolsky, and W. T. Vetterling (1989), *Numerical Recipes*, Cambridge Univ. Press, New York.
Reyners, M. (1980), A microearthquake study of the plate boundary, North Island, New Zealand, *Geophys. J. R. Astron. Soc.*, *64*, 1–22.
Reyners, M. (1989), New Zealand seismicity 1964–87: An interpretation, *N. Z. J. Geol. Geophys.*, *32*, 307–315.
Reyners, M. (1998), Plate coupling and the hazard of large subduction thrust earthquakes at the Hikurangi subduction zone, New Zealand, *N. Z. J. Geol. Geophys.*, *41*, 343–354.
Robinson, R. (1986), Seismicity, structure and tectonics of the Wellington region, New Zealand, *Geophys. J. R. Astron. Soc*, *87*, 379–409.
Rothacher, M., and G. L. Mader (1996), Combination of antenna phase center offsets and variations, Antenna calibration set: IGS_01, 30 June 1996, Int. GPS. Serv., Pasadena, Calif.
Rothacher, M., and L. Mervart (Eds.) (1996), Documentation of the Bernese GPS software version 4.0, 418 pp, Astron. Inst., Univ. of Bern, Bern, Switzerland.
Royden, L. H. (1993), Evolution of retreating subduction boundaries formed during continental collision, *Tectonics*, *12*, 629–638.
Savage, J. C. (1983), A dislocation model of strain accumulation and release at a subduction zone, *J. Geophys. Res.*, *88*, 4984–4996.

Schellart, W. P., G. S. Lister, and M. W. Jessell (2002), Analogue modelling of arc and backarc deformation in the New Hebrides and North Fiji Basin, *Geology*, *30*, 311–314.

Scholz, C. (1990), *The Mechanics of Earthquakes and Faulting*, 439 pp., Cambridge Univ. Press, New York.

Shemenda, A. I. (1993), Subduction of the lithosphere and back-arc dynamics: Insights from physical modeling, *J. Geophys. Res.*, *98*, 16,167–16,185.

Stern, T. A. (1987), Asymmetric back-arc spreading, heat flux and structure associated with the Central Volcanic Region of New Zealand, *Earth Planet. Sci. Lett.*, *85*, 265–276.

Stirling, M. W., G. H. McVerry, and K. R. Berryman (2002), A new seismic hazard model for New Zealand, *Bull. Seismol. Soc. Am.*, *92*, 1878–1903.

Taylor, B., and G. Karner (1983), On the evolution of marginal basins, *Rev. Geophys.*, *21*, 1727–1741.

Townsend, D., J. Begg, P. Villamor, and B. Lukovic (2002), Late Quaternary displacement of the Mokonui Fault, Wairarapa, New Zealand: A preliminary assessment of earthquake generating potential, *Client Rep.2002/58*, 30 pp., Inst. of Geol. and Nucl. Sci., Lower Hutt, N. Z.

Uyeda, S., and H. Kanamori (1979), Back-arc opening and mode of subduction, *J. Geophys. Res.*, *84*, 1049–1061.

Van Dissen, R., and K. R. Berryman (1996), Surface rupture earthquakes over the last ~1000 years in the Wellington region, New Zealand, and implications for ground shaking hazard, *J. Geophys. Res.*, *101*, 5999–6019.

Van Dissen, R., and R. S. Yeats (1991), Hope fault, Jordan thrust, and uplift of the Seaward Kaikoura Range, New Zealand, *Geology*, *19*, 393–396.

Van Dissen, R., K. R. Berryman, J. R. Pettinga, and N. L. Hill (1992), Paleoseismicity of the Wellington-Hutt Valley segment of the Wellington Fault, North Island, New Zealand, *N. Z. J. Geol. Geophys.*, *35*, 165–176.

Villamor, P., and K. R. Berryman (2001), A late Quaternary extension rate in the Taupo Volcanic Zone, New Zealand, derived from fault slip data, *N. Z. J. Geol. Geophys.*, *44*, 243–269.

Walcott, R. I. (1984), The kinematics of the plate boundary zone through New Zealand: A comparison of short- and long-term deformations, *Geophys. J. R. Astron. Soc.*, *79*, 613–633.

Wallace, L. M., C. Stevens, E. Silver, R. McCaffrey, W. Loratung, S. Hasiata, R. Stanaway, R. Curley, R. Rosa, and J. Taugaloidi (2004), GPS and seismological constraints on active tectonics and arc-continent collision in Papua New Guinea: Implications for mechanics of microplate rotations in a plate boundary zone, *J. Geophys. Res.*, *109*, B05404, doi:10.1029/2003JB002481.

Wang, K., and T. Dixon (2004), "Coupling" semantics and science in earthquake research, *Eos Trans. AGU*, *85*(18), 180.

Webb, T. H., and H. Anderson (1998), Focal mechanisms of large earthquakes in the North Island of New Zealand: Slip partitioning at an oblique active margin, *Geophys. J. Int.*, *134*, 40–86.

Wells, R. E., C. S. Weaver, and R. J. Blakely (1998), Fore-arc migration in Cascadia and its neotectonic significance, *Geology*, *26*, 759–762.

Wessel, P., and W. H. F. Smith (1995), New version of the Generic Mapping Tools released, *Eos Trans. AGU*, *76*, 329.

Williams, S. D. P., Y. Bock, P. Fang, P. Jamason, R. M. Nikolaidis, L. Prarwirodirdjo, M. Miller, and D. J. Johnson (2004), Error analysis of continuous GPS position time series, *J. Geophys. Res.*, *109*, B03412, doi:10.1029/2003JB002741.

Wilson, G. S., and D. M. McGuire (1995), Distributed deformation due to coupling across a subduction thrust: Mechanism of young tectonic rotation within the south Wanganui Basin, New Zealand, *Geology*, *23*, 645–648.

Wortel, M. J. R., and W. Spakman (2000), Subduction and slab detachment in the Mediterranean-Carpathian region, *Science*, *190*, 1910–1917.

Zachariasen, J., P. Villamor, J. Lee, B. Lukovic, and J. Begg (2000), Late Quaternary faulting of the Masterton and Carterton Faults, Wairarapa, New Zealand, *Client Rep.2000/70*, 35 pp., Inst. of Geol. and Nucl. Sci., Lower Hutt, N. Z.

Zhang, J., Y. Bock, H. Johnson, P. Fang, S. Williams, J. Genrich, S. Wdowinski, and J. Behr (1997), Southern California Permanent GPS Geodetic Array: Error analysis of daily position estimates and site velocities, *J. Geophys. Res.*, *102*, 18,035–18,055.

J. Beavan, D. Darby, and L. M. Wallace, Institute of Geological and Nuclear Sciences, 69 Gracefield Road, Lower Hutt, New Zealand. (l.wallace@gns.cri.nz)

R. McCaffrey, Department of Earth and Environmental Sciences, Rensselaer Polytechnic Institute, Troy, NY 12180-3590, USA.